13

Sparticle decays

Once sparticles are produced, they will typically decay into another sparticle together with SM particles via many different channels. The daughter sparticles subsequently decay to yet lighter sparticles until the decay cascade terminates in the stable LSP. In this discussion we have implicitly assumed that R-parity is conserved: otherwise, sparticles may also decay into just SM particles, and the final state would be comprised of only SM particles. However, whether or not R-parity is conserved, sparticle production at colliders typically leads to a variety of final state topologies via which to search for SUSY. Signal rates into any particular topology are determined by sparticle production cross sections studied in the last chapter, and by the branching fractions for various decays of sparticles.

In this chapter, we examine sparticle decays in the context of the R-parity conserving MSSM. As just mentioned, R-parity conservation implies that any sparticle decay chain will end in a stable LSP which may be a neutralino, a sneutrino, or, in models with local supersymmetry, also a gravitino. We have already seen in Chapter 9 that a sneutrino LSP is disfavored. A weak scale gravitino is essentially decoupled as far as collider physics considerations go. Hence, for most of this chapter, we will assume the gravitino is unimportant for sparticle decay calculations. However, as we saw in Section 11.3.1, an important exception to this occurs if the scale of SUSY breaking is low so that gravitinos are very light. To cover this possibility, we address sparticle decays to gravitinos in the last section of this chapter.

Before proceeding with the detailed examination of the decay rates and various branching fractions for individual sparticle decays, we pause to estimate the expected lifetimes for unstable sparticles. The lifetimes of sparticles are relevant when considering collider signatures for SUSY.

- Sparticles with lifetimes much longer than the time they take to traverse the detector will appear to be stable for the purposes of collider physics. If these are color and electrically neutral, they escape the detector unseen and manifest

https://doi.org/10.1017/9781009289801.014 Published online by Cambridge University Press

themselves as apparent missing energy and momentum in SUSY events. If such sparticles are electrically charged, they would cause ionization (the extent of which would depend on their velocity) and leave tracks in the detector, and would reveal themselves in experiments searching for heavy charged exotics. If these are electrically neutral but have strong interactions their experimental signatures may be quite complicated.[1] A particularly striking possibility is that such a particle may intermittently change into its charged partner by charged pion exchanges with nucleons in the experimental apparatus, and then back to neutral!

- Neutral sparticles with lifetimes somewhat shorter than their traversal time in the experimental apparatus would result in displaced vertices. Such a sparticle would be produced at the primary vertex, but would travel a macroscopic distance before decaying at a secondary vertex, which may, depending on the lifetime, be quite distant from the primary interaction point. Experimentalists searching for new physics should keep this possibility in mind, and not discard such an exotic signal as due to background from secondary (cosmic ray) interactions or other noise. If the sparticle lifetime is comparable to B meson lifetimes, SUSY events would contain displaced vertices (with tracks not pointing back to the primary interaction point) that would be identified in specialized microvertex detectors that are an integral part of most contemporary general purpose detectors.
- Finally, sparticles with lifetimes too short to yield displaced vertices that can be resolved by the microvertex detectors would appear to decay promptly at the primary vertex. A familiar SM example of such a situation is the production and decay of the W or Z bosons. In this case, we can get a handle on sparticle properties only by studying their decay products.

The partial decay rate for a particle decaying via $A \to a_1 + a_2 + \cdots + a_n$ is given in the rest frame of A by,

$$\Gamma_n = (2\pi)^{4-3n} \frac{1}{2M_A} \int \frac{\mathrm{d}^3 p_{a_1}}{2E_{a_1}} \cdots \frac{\mathrm{d}^3 p_{a_n}}{2E_{a_n}} |\mathcal{M}(A \to a_1 a_2 \cdots a_n)|^2 \times \delta^4(P_A - P_{a_1} - P_{a_2} \cdots - P_{a_n}), \tag{13.1a}$$

where, for any sparticle A, the spin and color summed and averaged squared matrix element $|\mathcal{M}|^2$ for the decay is evaluated using the matrix element obtained using the sparticle interactions listed in Chapter 8. The *total decay rate* is then obtained by summing the partial decay rates for all possible decay modes of A. The lifetime of A is the inverse of this total decay rate,

$$\tau_A = \frac{1}{\sum_n \Gamma_n}. \tag{13.1b}$$

[1] The elementary sparticle may well be charged and colored, but may bind with SM quarks to produce an unconfined strongly interacting, electrically neutral "meson" that traverses the apparatus.

https://doi.org/10.1017/9781009289801.014 Published online by Cambridge University Press

The mass dimension of the matrix element $\mathcal{M}$ that appears in (13.1a) can readily be checked to be $[\mathcal{M}] = 3 - n$. The matrix element for two-body decays has dimensions of mass, that for three-body decays is dimensionless, etc.

Before proceeding to evaluate the partial widths for the various decays of individual sparticles, let us estimate their order of magnitude. For two-body decays of unpolarized particles, Lorentz invariance implies that the squared matrix element, summed over final state spins, must be independent of final state momenta: i.e. it is constant.[2] This constant must generically be $\sim k^2 \times m_A^2$ where k is the coupling constant in the interaction responsible for the decay $A \to a_1 a_2$.[3] Using

$$\int \delta^4(P_A - P_{a_1} - P_{a_2}) \frac{\mathrm{d}^3 p_{a_1}}{2E_{a_1}} \frac{\mathrm{d}^3 p_{a_2}}{2E_{a_2}} = \frac{\pi \lambda^{1/2}(m_A^2, m_{a_1}^2, m_{a_2}^2)}{2m_A^2}, \tag{13.2a}$$

it is easy to check that the partial width for the decay,

$$\begin{aligned} \Gamma(A \to a_1 a_2) &\sim \frac{f}{4m_A} \frac{k^2}{4\pi} \lambda^{1/2}(m_A^2, m_{a_1}^2, m_{a_2}^2) \\ &\simeq f \frac{k^2}{4\pi} \frac{m_A}{4}, \end{aligned} \tag{13.2b}$$

where f includes spin and color factors, and in the last step we have ignored any phase space suppression for the decay. The point of this calculation is to show that if the coupling k is comparable to the electromagnetic coupling or larger, the typical width of a 100 GeV particle undergoing two-body decays is $\gtrsim 200$ MeV for a single channel, corresponding to a lifetime $\lesssim 10^{-23}$ seconds: frequently, the total decay rate is considerably larger because of color factors and also because there are several channels. Clearly, such lifetimes are orders of magnitude too short to be detectable by even the best vertex detectors. As shown in the exercise below, the same conclusion obtains if sparticles dominantly decay via three-body decays mediated by gauge interactions.

In the subsequent sections, we will see that essentially all MSSM sparticles can decay (at tree level) via two- or three-body decays mediated by SM gauge interactions. We conclude that, except in very special cases where there is severe phase space suppression, sparticles decay promptly in the experimental apparatus. Important exceptions may occur in GMSB models where the NLSP decays into a (longitudinal) gravitino via suppressed couplings as discussed in Section 11.3.1, or for the case of R-parity violating models where the lightest dominantly R-odd

[2] The matrix element can be a function of scalar products of various momenta which, by momentum conservation can be written in terms of particle masses.

[3] We assume that the interaction does not have any special features that forbids the appearance of the parent's mass in the matrix element. An example where this is forbidden is the matrix element for charged pion decay which, because of chiral symmetry, has to be proportional to the final state fermion mass rather than m_π.

https://doi.org/10.1017/9781009289801.014 Published online by Cambridge University Press

particle decays via very small R-parity violating couplings. These special situations will be treated separately.

In the rest of this chapter we will focus on the decay patterns of various sparticles since these determine the event topologies via which to search for supersymmetry at high energy colliders. We illustrate the calculation of partial decay widths by evaluating the width for three-body decays of the gluino. In Appendix B, we list formulae for widths of all tree-level two-body sparticle decay modes along with formulae for the important three-body decay widths.

Exercise *Estimate the order of magnitude of the partial width for a three-body decay of A and show that if this decay is mediated by gauge couplings, we should not expect a discernible secondary vertex in the experimental apparatus. Proceed by the following steps.*

(a) *Although the matrix element for three-body decays is not a constant but depends on the final state momenta, we may estimate its order of magnitude. If the decay is mediated by a virtual bosonic sparticle, the amplitude will contain a propagator of this heavy bosonic particle. Convince yourself that the order of magnitude of the matrix element (which we saw must be dimensionless) is given by,*

$$|\mathcal{M}|^2 \sim k_1^2 k_2^2 \left(\frac{m_A^2}{m_H^2}\right)^2,$$

where k_1 and k_2 are the dimensionless couplings at each of the two vertices involving the virtual heavy particle of mass m_H. Here, m_H^2 in the denominator comes from the propagator, and the m_A^2 is inserted to make the matrix element dimensionless.

(b) *Neglecting any masses for the final state particles, show that the partial width for the three-body decay is then given by,*

$$\Gamma(A \to a_1 a_2 a_3) \sim \frac{f}{32\pi}\left(\frac{k_1 k_2}{4\pi}\right)^2 \frac{m_A^5}{m_H^4},$$

where f again contains spin and color factors.

(c) *Assuming that the mass of the virtual sparticle is no more than an order of magnitude larger than that of the decaying parent, estimate the partial width for this decay, taking the couplings k_1 and k_2 to be comparable to gauge couplings.*

(d) *Frequently, each sparticle has several three-body decay modes, so that the total decay rate is enhanced by color and multiplicity factors. Convince yourself that the lifetime of a 100 GeV sparticle decaying via SM gauge interactions is typically smaller than $\sim 10^{-16}$ seconds.*

https://doi.org/10.1017/9781009289801.014 Published online by Cambridge University Press

Note that if the virtual sparticle is a fermion, the matrix element may have just one power of m_H in the denominator, in which case the expected lifetime would be even smaller.

13.1 Decay of the gluino

If the gluino is heavy enough, it can decay via the strong interaction to quark plus squark. Neglecting intergenerational mixing, the possible two-body decays are:

$$\tilde{g} \to u\bar{\tilde{u}}_{\rm L},\ \bar{u}\tilde{u}_{\rm L},\ u\bar{\tilde{u}}_{\rm R},\ \bar{u}\tilde{u}_{\rm R}, \tag{13.3a}$$
$$\to d\bar{\tilde{d}}_{\rm L},\ \bar{d}\tilde{d}_{\rm L},\ d\bar{\tilde{d}}_{\rm R},\ \bar{d}\tilde{d}_{\rm R}, \tag{13.3b}$$
$$\to s\bar{\tilde{s}}_{\rm L},\ \bar{s}\tilde{s}_{\rm L},\ s\bar{\tilde{s}}_{\rm R},\ \bar{s}\tilde{s}_{\rm R}, \tag{13.3c}$$
$$\to c\bar{\tilde{c}}_{\rm L},\ \bar{c}\tilde{c}_{\rm L},\ c\bar{\tilde{c}}_{\rm R},\ \bar{c}\tilde{c}_{\rm R}, \tag{13.3d}$$
$$\to b\bar{\tilde{b}}_1,\ \bar{b}\tilde{b}_1,\ b\bar{\tilde{b}}_2,\ \bar{b}\tilde{b}_2, \quad \text{and} \tag{13.3e}$$
$$\to t\bar{\tilde{t}}_1,\ \bar{t}\tilde{t}_1,\ t\bar{\tilde{t}}_2,\ \bar{t}\tilde{t}_2. \tag{13.3f}$$

Each flavor combination must be separately calculated, since the different squark types will have different decay modes, and each decay chain can give rise to distinct final states and ensuing signatures. Unless they are kinematically suppressed these two-body decays generally dominate other decays. Their partial widths are given by (B.1a) and (B.1b) of Appendix B.

Since the gluino has only strong interactions, if these two-body decays to squarks are kinematically forbidden, then the gluino would dominantly decay to charginos and neutralinos via three-body decays mediated by virtual squarks. Again neglecting inter-generational mixing, the possible decays are,

$$\tilde{g} \to u\bar{u}\widetilde{Z}_i,\ d\bar{d}\widetilde{Z}_i,\ s\bar{s}\widetilde{Z}_i,\ c\bar{c}\widetilde{Z}_i,\ b\bar{b}\widetilde{Z}_i,\ t\bar{t}\widetilde{Z}_i, \tag{13.4a}$$
$$\to u\bar{d}\widetilde{W}_j^-,\ \bar{u}d\widetilde{W}_j^+,\ c\bar{s}\widetilde{W}_j^-,\ \bar{c}s\widetilde{W}_j^+,\ t\bar{b}\widetilde{W}_j^-,\ \bar{t}b\widetilde{W}_j^+, \tag{13.4b}$$

where $i = 1$–4 and $j = 1,\ 2$. Note that in all models with a neutralino LSP, the decays $\tilde{g} \to q\bar{q}\widetilde{Z}_1$ are kinematically allowed ($q = u, d, s, c$). As an example calculation, we will illustrate gluino three-body decay to a pair of light quarks plus a chargino.

13.1.1 $\tilde{g} \to u\bar{d}\widetilde{W}_j$: a worked example

At leading order, the $\tilde{g} \to u\bar{d}\widetilde{W}_j$ decay occurs via the Feynman diagrams shown in Fig. 13.1. The decay amplitude for diagram (1) is constructed from

$$\langle u_a \bar{d}_b \widetilde{W}_j | T \left[\left(-\sqrt{2} g_s (\mathrm{i})^{\theta_{\tilde{g}}} \tilde{u}_{\rm L} \bar{u} P_{\rm R} \frac{\lambda_B}{2} \tilde{g}_B(x) \right) \cdot \left(\mathrm{i} A^d_{\widetilde{W}_j} \tilde{u}^\dagger_{\rm L} \overline{\widetilde{W}}_i P_{\rm L} d(y) \right) \right] | \tilde{g}_A \rangle,$$

https://doi.org/10.1017/9781009289801.014 Published online by Cambridge University Press

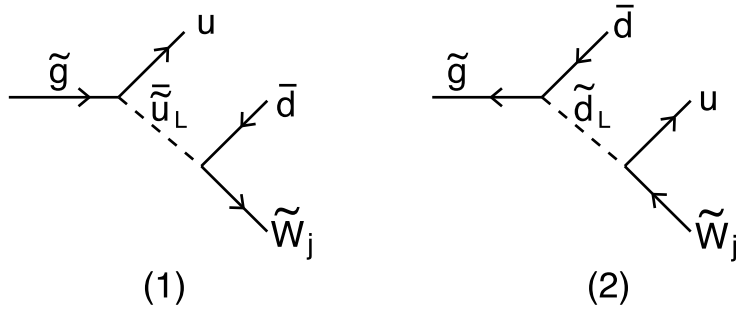

Figure 13.1 Feynman diagrams contributing to the decay $\tilde{g} \to u\bar{d}\widetilde{W}_j$.

where a, b, and A denote the color indices of the final state quarks and the decaying gluino. The matrix element can be evaluated as described in the last chapter. The external particles can be reduced using the creation/annihilation operators; again the exponential wave function factors lead to momentum conservation at each vertex. Finally, the $\tilde{u}_{\rm L}$ and $\tilde{u}_{\rm L}^\dagger$ fields contract together to yield a $\tilde{u}_{\rm L}$ propagator factor $D_F(\tilde{u}_{\rm L}) = \frac{1}{(\tilde{g}-u)^2 - m^2_{\tilde{u}_{\rm L}}}$. Following the steps detailed in Chapter 12, we omit irrelevant factors of i, and find that the matrix element is given by,

$$\mathcal{M}_1 = -\mathrm{i}(\mathrm{i})^{\theta_{\tilde{g}}}\sqrt{2}g_s A^d_{\widetilde{W}_j}\frac{\lambda_{Aab}}{2}\bar{u}(u)P_{\rm R}u(\tilde{g})\cdot D_F(\tilde{u}_{\rm L})\cdot\bar{u}(\widetilde{W}_j)P_{\rm L}v(\bar{d}). \qquad (13.5a)$$

The sum and average over color indices yields a factor

$$\frac{1}{8}\sum_A \frac{\lambda_{Aab}}{2}\frac{\lambda^*_{Aab}}{2} = \frac{1}{8}\mathrm{Tr}\frac{\lambda_A}{2}\frac{\lambda_A}{2} = \frac{1}{8}\frac{1}{2}\delta_{AA} = \frac{1}{2},$$

where in the second step we have used the Hermiticity of the $SU(3)$ generators. Using usual trace techniques, the sum and average over colors and spins then yields the squared matrix element,

$$\frac{1}{2}\frac{1}{8}\sum|\mathcal{M}_1|^2 = 2g_s^2|A^d_{\widetilde{W}_j}|^2\frac{\tilde{g}\cdot u\ \widetilde{W}_j\cdot\bar{d}}{[(\tilde{g}-u)^2 - m^2_{\tilde{u}_{\rm L}}]^2}. \qquad (13.5b)$$

A similar calculation for diagram (2) yields the matrix element,

$$\mathcal{M}_2 = -\mathrm{i}(-\mathrm{i})^{\theta_{\tilde{g}}}\sqrt{2}g_s A^{u*}_{\widetilde{W}_j}\frac{\lambda_{Aab}}{2}\bar{v}(\tilde{g})P_{\rm L}v(\bar{d})\cdot D_F(\tilde{d}_{\rm L})\cdot\bar{u}(u)P_{\rm R}v(\widetilde{W}_j), \qquad (13.6a)$$

where the chargino is treated as an antiparticle since its interaction with the down squark is written in terms of the field $\widetilde{W}^c_j$. This explains the direction of the arrow on the chargino line in diagram (2) of Fig. 13.1; we will leave it to the reader to check the reason for the reversal of the corresponding arrow on the gluino line. We

https://doi.org/10.1017/9781009289801.014 Published online by Cambridge University Press

then obtain the spin and color averaged squared matrix element,

$$\frac{1}{2}\frac{1}{8}\sum|\mathcal{M}_2|^2 = 2g_s^2|A^u_{\widetilde{W}_j}|^2\frac{\tilde{g}\cdot\bar{d}\;\widetilde{W}_j\cdot u}{[(\tilde{g}-\bar{d})^2-m^2_{\tilde{d}_{\rm L}}]^2}. \tag{13.6b}$$

Finally, we turn to the interference term,

$$\begin{aligned}\mathcal{M}_1\mathcal{M}_2^\dagger = (-1)^{\theta_{\tilde{g}}}2g_s^2A^d_{\widetilde{W}_j}A^u_{\widetilde{W}_j}(\frac{\lambda_A}{2})_{ab}(\frac{\lambda_A^*}{2})_{ab}D_F(\tilde{u}_{\rm L})D_F(\tilde{d}_{\rm L})\\ \times\bar{u}(u)P_{\rm R}u(\tilde{g})\cdot\bar{v}(\bar{d})P_{\rm R}v(\tilde{g})\cdot\bar{u}(\widetilde{W}_j)P_{\rm L}v(\bar{d})\cdot\bar{v}(\widetilde{W}_j)P_{\rm L}u(u).\end{aligned}$$

Just as in the evaluation of the interference term following (12.4c), we find a mismatch between spinors involving the $\tilde{g}$ and also the $\widetilde{W}_j$. As before, this can be rectified using the relations $u = C\bar{v}^T$ and $v = C\bar{u}^T$, which yield:

$$\begin{aligned}\bar{v}(\bar{d})P_{\rm R}v(\tilde{g}) = u^T(\bar{d})C\,P_{\rm R}C\bar{u}^T(\tilde{g}) = -\bar{u}(\tilde{g})P_{\rm R}u(\bar{d}), \quad \text{and}\\ \bar{u}(\widetilde{W}_j)P_{\rm L}v(\bar{d}) = v^T(\widetilde{W}_j)C\,P_{\rm L}C\bar{u}^T(\bar{d}) = -\bar{u}(\bar{d})P_{\rm L}v(\widetilde{W}_j).\end{aligned}$$

Then the spin and color summed and averaged interference term becomes,

$$\frac{1}{8}\frac{1}{2}\sum(\mathcal{M}_1\mathcal{M}_2^\dagger + \quad \text{c.c.}) = -\frac{2g_s^2(-1)^{\theta_{\tilde{g}}}m_{\tilde{g}}m_{\widetilde{W}_j}\,\mathrm{Re}(A^d_{\widetilde{W}_j}A^u_{\widetilde{W}_j})u\cdot\bar{d}}{[(\tilde{g}-u)^2-m^2_{\tilde{u}_{\rm L}}][(\tilde{g}-\bar{d})^2-m^2_{\tilde{d}_{\rm L}}]}. \tag{13.6c}$$

The width for the decay $\tilde{g}\to u\bar{d}\widetilde{W}_j$ can now be obtained using (13.1a) and integrating over the entire phase space. To integrate $\sum|\mathcal{M}_1|^2$, we first re-write the dot product $\widetilde{W}_j\cdot\bar{d} = (Q^2 - m^2_{\widetilde{W}_j} - m^2_{\bar{d}})/2$, with $Q = \widetilde{W}_j + \bar{d} = \tilde{g} - u$, so that the integrand is independent of $\widetilde{W}_j$ and $\bar{d}$. The integration over the momenta of $\widetilde{W}_j$ and $\bar{d}$ can be easily performed using the invariant scalar integral (13.2a) leaving just the integral over the three momentum of the u quark to be performed. It is most convenient to write the integrand in the rest frame of the gluino. The measure $\mathrm{d}^3u/2E_u = 2\pi|\vec{p}_u|\mathrm{d}E_u$ so that the contribution to the partial width from $|\mathcal{M}_1|^2$ is

$$\Gamma_{11} = \frac{\alpha_s|A^d_{\widetilde{W}_j}|^2}{16\pi^2}\psi(m_{\tilde{g}}, m_{\tilde{u}_{\rm L}}, m_{\widetilde{W}_j}), \tag{13.7a}$$

where

$$\psi(m_{\tilde{g}}, m_{\tilde{q}}, m) = \int\mathrm{d}E\frac{E^2(m^2_{\tilde{g}} - 2m_{\tilde{g}}E - m^2)^2}{(m^2_{\tilde{g}} - 2m_{\tilde{g}}E - m^2_{\tilde{q}})^2(m^2_{\tilde{g}} - 2m_{\tilde{g}}E)}, \tag{13.7b}$$

and where the limits of integration (neglecting the u quark mass) range from $E_{\rm min} = 0$ to $E_{\rm max} = (m^2_{\tilde{g}} - m^2)/2m_{\tilde{g}}$. Similarly, integrating $\sum|\mathcal{M}_2|^2$ over the phase space

https://doi.org/10.1017/9781009289801.014 Published online by Cambridge University Press

gives,

$$\Gamma_{22} = \frac{\alpha_s |A^u_{\widetilde{W}_j}|^2}{16\pi^2} \psi(m_{\tilde{g}}, m_{\tilde{d}_L}, m_{\widetilde{W}_j}). \tag{13.7c}$$

Finally, we must integrate over the interference term. Since this term involves $\tilde{g} \cdot u$ and $\tilde{g} \cdot \bar{d}$ dot products in the propagator denominators, we cannot use covariant scalar, vector or tensor integrals in its evaluation. Instead, we will evaluate the three-body phase space integral directly. Toward this end, we write

$$\frac{\mathrm{d}^3 \widetilde{W}_j}{2E_{\widetilde{W}_j}} = \mathrm{d}^4 \widetilde{W}_j \theta(\widetilde{W}^0_j) \delta(\widetilde{W}^2_j - m^2_{\widetilde{W}_j}),$$

and use the energy–momentum conserving δ-function to integrate over the chargino four-momentum. Since $\widetilde{W}_j = \tilde{g} - u - \bar{d}$, the step function $\theta(\widetilde{W}^0_j)$ is just one (because of limits on the particle energies obtained below). The remaining integrand can then be written in the rest frame of the gluino with the u quark direction chosen as the z-axis. The δ-function that specifies the chargino to be on its mass shell can be then written as,

$$\delta\left[(\tilde{g} - u - \bar{d})^2 - m^2_{\widetilde{W}_j}\right] = \frac{1}{2E_u E_{\bar{d}}} \delta\left[1 - \cos\theta + \frac{m^2_{\tilde{g}} - m^2_{\widetilde{W}_j} - 2m_{\tilde{g}}(E_u + E_{\bar{d}})}{2E_u E_{\bar{d}}}\right],$$

where θ is the angle between the up and down quark momenta. Neglecting quark masses, it is now straightforward to see that

$$\begin{aligned}
&\int \frac{u \cdot \bar{d}}{[(\tilde{g} - u)^2 - m^2_{\tilde{u}_L}][(\tilde{g} - \bar{d})^2 - m^2_{\tilde{d}_L}]} \delta^4(\tilde{g} - \widetilde{W}_j - u - \bar{d}) \frac{\mathrm{d}^3 u}{2E_u} \frac{\mathrm{d}^3 \bar{d}}{2E_{\bar{d}}} \frac{\mathrm{d}^3 \widetilde{W}_j}{2E_{\widetilde{W}_j}} \\
&\quad = \pi^2 \int \frac{u \cdot \bar{d}\, \mathrm{d}E_u \mathrm{d}E_{\bar{d}}}{[(\tilde{g} - u)^2 - m^2_{\tilde{u}_L}][(\tilde{g} - \bar{d})^2 - m^2_{\tilde{d}_L}]} \\
&\quad = -\frac{\pi^2}{2} \int \frac{\mathrm{d}E_u}{(m^2_{\tilde{g}} - 2m_{\tilde{g}} E_u - m^2_{\tilde{u}_L})} \int \mathrm{d}E_{\bar{d}} \left(1 + \frac{m^2_{\tilde{d}_L} - m^2_{\widetilde{W}_j} - 2m_{\tilde{g}} E_u}{m^2_{\tilde{g}} - 2m_{\tilde{g}} E_{\bar{d}} - m^2_{\tilde{d}_L}}\right).
\end{aligned}$$

The integration over $\mathrm{d}E_{\bar{d}}$ is simple, once the limits of integration are determined (see the exercise below). We then find that the contribution to the width from the interference term takes the form,

$$\Gamma_{12} = \frac{-\alpha_s (-1)^{\theta_{\tilde{g}}} \mathrm{Re}(A^u_{\widetilde{W}_j} A^d_{\widetilde{W}_j})}{8\pi^2} \phi(m_{\tilde{g}}, m_{\tilde{u}_L}, m_{\tilde{d}_L}, m_{\widetilde{W}_j}), \tag{13.8a}$$

https://doi.org/10.1017/9781009289801.014 Published online by Cambridge University Press

where

$$\phi(m_{\tilde{g}}, m_{\tilde{u}_L}, m_{\tilde{d}_L}, m) = \frac{m}{2}\int \frac{\mathrm{d}E_u}{m_{\tilde{g}}^2 - m_{\tilde{u}_L}^2 - 2m_{\tilde{g}}E_u}\left[\frac{-E_u(m_{\tilde{g}}^2 - m^2 - 2m_{\tilde{g}}E_u)}{m_{\tilde{g}}(m_{\tilde{g}} - 2E_u)} - \frac{2m_{\tilde{g}}E_u - m_{\tilde{d}_L}^2 + m^2}{2m_{\tilde{g}}}\log\frac{m_{\tilde{d}_L}^2(m_{\tilde{g}} - 2E_u) - m_{\tilde{g}}m^2}{(m_{\tilde{g}} - 2E_u)(m_{\tilde{d}_L}^2 - 2m_{\tilde{g}}E_u - m^2)}\right], \quad (13.8b)$$

with the range of integration from 0 to $(m_{\tilde{g}}^2 - m^2)/2m_{\tilde{g}}$. The partial decay width is then given by

$$\Gamma(\tilde{g} \to u\bar{d}\widetilde{W}_j) = \Gamma_{11} + \Gamma_{22} + \Gamma_{12}. \quad (13.9)$$

By CP invariance, $\Gamma(\tilde{g} \to u\bar{d}\widetilde{W}_j^-) = \Gamma(\tilde{g} \to d\bar{u}\widetilde{W}_j^+)$. This will lead to an important signature for gluinos. Moreover, these partial widths are generation-independent as long as quark Yukawa interactions can be neglected. For decays to third generation quarks the calculation is considerably more complicated mainly because the higgsino components of the charginos also couple via Yukawa interactions. Moreover, intra-generational squark mixing and final state quark masses also need to be taken into account. The formula for this partial width is given in Section B.1.4 of Appendix B.

Exercise *The requirement that* $|\cos\theta| \leq 1$ *determines the limits on the energy of the down quark. Using the value of* $\cos\theta$ *given by the chargino mass shell* δ*-function, show that*

$$E_{\bar{d}}(\min) = (m_{\tilde{g}}^2 - m_{\widetilde{W}_j}^2 - 2m_{\tilde{g}}E_u)/2m_{\tilde{g}},$$
$$E_{\bar{d}}(\max) = (m_{\tilde{g}}^2 - m_{\widetilde{W}_j}^2 - 2m_{\tilde{g}}E_u)/2(m_{\tilde{g}} - 2E_u).$$

The limits on the up quark energy are even easier to determine. In the gluino rest frame, if u *is produced at rest, then* $E_u(\min) = 0$*, while if* $\bar{d}$ *is produced at rest, then* $E_u(\max) = (m_{\tilde{g}}^2 - m_{\widetilde{W}_j}^2)/2m_{\tilde{g}}$.

Work out how these limits are modified if quarks have non-zero masses. This is relevant for the decay $\tilde{g} \to t\bar{b}\widetilde{W}_j$.

13.1.2 Other gluino decays

We have already mentioned that the decays $\tilde{g} \to c\bar{s}\widetilde{W}_j^-$ and $\tilde{g} \to t\bar{b}\widetilde{W}_j^-$ (along with the corresponding CP conjugate decays) may also occur. If the latter decay is kinematically unsuppressed, its partial width may be considerably larger than that

https://doi.org/10.1017/9781009289801.014 Published online by Cambridge University Press

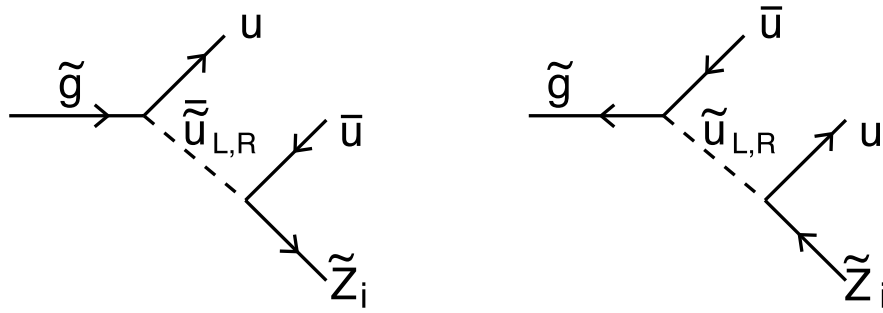

Figure 13.2 Feynman diagrams contributing to the decay $\tilde{g} \to u\bar{u}\widetilde{Z}_i$. Decays to other flavors of squarks occur via similar diagrams.

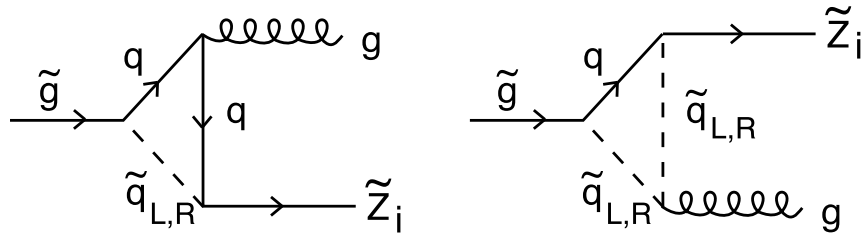

Figure 13.3 Feynman diagrams contributing to the decay $\tilde{g} \to g\widetilde{Z}_i$. Since the gluino and the neutralino are Majorana particles, these same diagrams but with reversed arrows also contribute to the amplitude. This corresponds to distinct contractions in the evaluation of the decay matrix element.

for three-body decays to light squarks. This occurs in part because the top (and for large $\tan\beta$, bottom) quark Yukawa couplings are large, and also because in all models where squark mass parameters are (roughly) equal at some high scale, the physical masses of light bottom and top squarks are significantly smaller than first and second generation squark masses.

Gluinos can also decay via three-body mode to neutralinos. The diagrams contributing to $\tilde{g} \to u\bar{u}\widetilde{Z}_i$ are shown in Fig. 13.2. The calculation of the decay width is very similar to the one illustrated for $\tilde{g} \to u\bar{d}\widetilde{W}_j$. For decays to massless quarks, the chiral structure of the interaction ensures that there is no interference term between diagrams involving left- and right-squark exchange. The corresponding partial width is given by Eq. (B.4). The decays $\tilde{g} \to b\bar{b}\widetilde{Z}_i$ and $\tilde{g} \to t\bar{t}\widetilde{Z}_i$ may also occur. Once again, the evaluation of these partial widths is complicated because Yukawa couplings, squark mixing, and quark masses have all to be included. The relevant formulae can be found in Section B.1.3 of Appendix B.

It is also possible for the gluino to decay via loop diagrams as $\tilde{g} \to g\widetilde{Z}_i$, as shown in Fig. 13.3. Each diagram is separately divergent but the summed amplitude is finite

https://doi.org/10.1017/9781009289801.014 Published online by Cambridge University Press

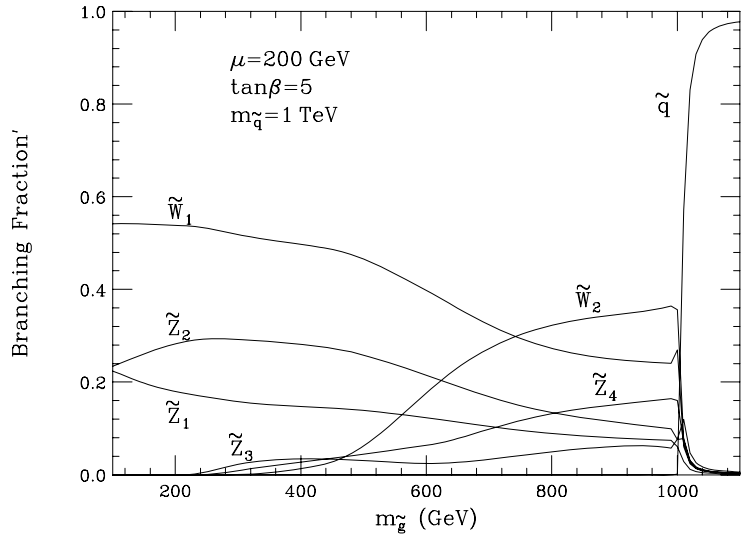

Figure 13.4 Branching fractions for $\tilde{g}$ decay to $q\bar{q}\widetilde{Z}_i$, $q\bar{q}'\widetilde{W}_j$, and $q\tilde{q}$ final states as a function of $m_{\tilde{g}}$ for MSSM model parameters shown.

as it must be in a renormalizable theory. Since the amplitude has an additional factor of the strong coupling relative to the amplitudes for tree-level three-body decays as well as a loop suppression factor, the partial width for this decay is usually smaller than that for three-body tree-level decays. However, in some regions of MSSM parameter space, this decay mode can be significant, since it can be enhanced by third generation Yukawa couplings, and suffers less kinematic suppression. We do not list the formula for this decay here but refer the reader to the literature.[4]

In Fig. 13.4, we show gluino branching ratios to charginos and neutralinos as a function of $m_{\tilde{g}}$, for degenerate soft SUSY breaking squark masses of $m_{\tilde{q}} = 1$ TeV, with $\mu = 200$ GeV, and $\tan\beta = 5$, in the MSSM with gaugino mass unification. Values of $m_{\tilde{g}} \lesssim 550$ GeV are excluded by the LEP constraint on the chargino mass. However, we should understand that this figure is for illustrative purposes only. Two-body gluino decays are kinematically forbidden over most of the range of $m_{\tilde{g}}$ in the figure. For low values of $m_{\tilde{g}}$, $\widetilde{Z}_1$, $\widetilde{Z}_2$, and $\widetilde{W}_1$ are all extremely light, and the gluino decays mainly via three-body modes into $q\bar{q}'\widetilde{W}_1$, $q\bar{q}\widetilde{Z}_1$, and $q\bar{q}\widetilde{Z}_2$. Moreover, we see that the branching fraction to the kinematically favored $q\bar{q}\widetilde{Z}_1$ mode is smaller than that for gluino decays to the heavier neutralino $\widetilde{Z}_2$ or to the chargino. The reason is that for low values of $m_{\tilde{g}}$, $2M_1 \simeq M_2 \simeq m_{\tilde{g}}/3 \ll \mu$, so that the lightest neutralino is dominantly a bino while $\widetilde{Z}_2$ and $\widetilde{W}_1$ are dominantly winos. Since the $SU(2)_{\rm L}$ gauge coupling is larger than the hypercharge gauge coupling, decays to the bino-like LSP are dynamically suppressed. The partial width for the decay to a chargino is almost

[4] See e.g., H. Baer, X. Tata and J. Woodside, *Phys. Rev.* **D42**, 1568 (1990).

https://doi.org/10.1017/9781009289801.014 Published online by Cambridge University Press

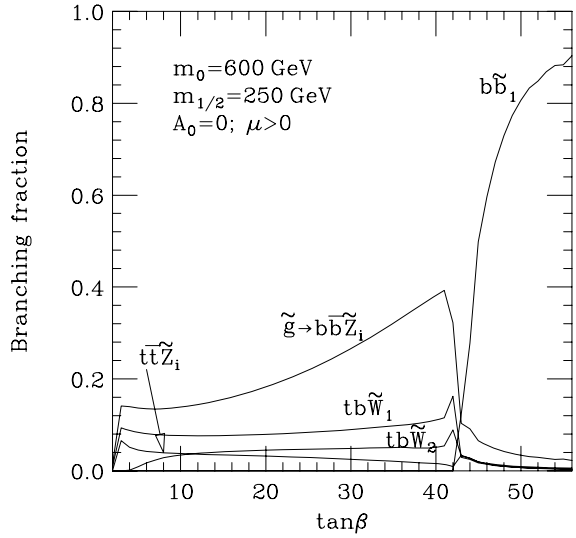

Figure 13.5 Branching fractions of the $\tilde{g}$ to final states involving third generation quarks versus $\tan\beta$ in the mSUGRA model. Also shown is the total branching fraction for decays to quarks of the first two generations.

twice that to $\widetilde{Z}_2$; this is reasonable because there are two charged wino states and just one neutral wino state. Decays to heavy neutralinos and the heavier chargino (which are mainly higgsino-like) are kinematically and dynamically suppressed. As $m_{\tilde{g}}$ increases, decays to states including heavier charginos and neutralinos become possible. Ultimately, these dominate the branching fractions. This is because for fixed μ, M_1 and M_2 increase with $m_{\tilde{g}}$ so that for very heavy gluinos, it is the heavier chargino $\widetilde{W}_2$ and the heavier neutralinos $\widetilde{Z}_3$ and $\widetilde{Z}_4$ that are mainly gaugino-like and so have large couplings to the quark–squark system: decays to the more higgsino-like $\widetilde{W}_1$, $\widetilde{Z}_1$, and $\widetilde{Z}_2$, though kinematically favored are suppressed by mixing angles. That heavy gluinos decay to heavy charginos and neutralinos which subsequently decay to lighter charginos and neutralinos is quite a general feature of SUSY models. Of course, as we can see, if $m_{\tilde{g}} > (m_q + m_{\tilde{q}})$, then the two-body decays to quark plus squark become kinematically accessible and rapidly dominate the branching fraction. Since these occur via only strong interactions which are flavor independent, aside from mass effects, every flavor and type of squark will be democratically produced.

In Fig. 13.5, we show the $\tilde{g}$ branching fractions to states including third generation quarks, as a function of $\tan\beta$, in the mSUGRA model for $m_0 = 600$ GeV, $m_{1/2} = 250$ GeV, $A_0 = 0$, and $\mu > 0$. For small values of $\tan\beta$ just the top quark Yukawa coupling is important, but decays to t quarks are somewhat suppressed by phase space. As $\tan\beta$ increases, the magnitude of the bottom (and also tau) Yukawa coupling increases; as a result, $m_{\tilde{b}_1}$ is decreased both because of

https://doi.org/10.1017/9781009289801.014 Published online by Cambridge University Press

renormalization group evolution as well as left-right mixing. Thus as $\tan\beta$ increases, gluino decays to bottom quarks become increasingly important both due to direct Yukawa couplings at the chargino and neutralino vertices, as well as to propagator enhancement. As can be seen from the figure, gluino production events at hadron colliders should be rich in b-quark jets if the parameter $\tan\beta$ is large. Moreover, the primary b-quark jets should be very hard, and events with hard b-jets and large $E_{\rm T}^{\rm miss}$ may give a striking signature at the LHC.[5] If $\tan\beta$ is large enough ($\tan\beta \gtrsim 42$ in our illustration), the decays $\tilde{g} \to b\bar{b}\tilde{b}_1$ and $\bar{b}\tilde{b}_1$ become kinematically accessible, and rapidly dominate the gluino decay rate. In some cases, the momentum distribution of the b-jets from the decay of the gluino and the $\tilde{b}_1$ squark can even provide information about their masses.

13.2 Squark decays

Squarks dominantly decay via two-body modes. The decay $\tilde{q}_i \to q\widetilde{Z}_1$ is kinematically accessible by assumption as long as the mass of the daughter quark is negligible. For the first generation, Yukawa couplings can be neglected and possible decay modes include,

$$\tilde{u}_{\rm L} \to u\widetilde{Z}_i,\ d\widetilde{W}_j^+,\ u\tilde{g}, \tag{13.10a}$$

$$\tilde{d}_{\rm L} \to d\widetilde{Z}_i,\ u\widetilde{W}_j^-,\ d\tilde{g}, \tag{13.10b}$$

$$\tilde{u}_{\rm R} \to u\widetilde{Z}_i,\ u\tilde{g}, \tag{13.10c}$$

$$\tilde{d}_{\rm R} \to d\widetilde{Z}_i,\ d\tilde{g}. \tag{13.10d}$$

Notice that right-squarks have no coupling to charginos, and so can only decay to $\tilde{g}$ or $\widetilde{Z}_i$. The decay modes for $\tilde{c}_{\rm L}$, $\tilde{c}_{\rm R}$, $\tilde{s}_{\rm L}$ and $\tilde{s}_{\rm R}$ are similar. Unless they are kinematically suppressed, decays to gluinos dominate. Partial widths for two-body decays of squarks to gluinos, charginos, and neutralinos may be found in Appendix B.2.

For third generation squarks, squark mixing effects as well as non-negligible Yukawa couplings lead to more complicated decay patterns. Bottom squarks may decay via the following modes, if these are kinematically accessible:

$$\tilde{b}_{1,2} \to b\tilde{g},\ b\widetilde{Z}_i,\ t\widetilde{W}_j,\ W\tilde{t}_{1,2},\ H^-\tilde{t}_{1,2} \quad \text{and} \tag{13.11a}$$

$$\tilde{b}_2 \to Z\tilde{b}_1,\ h\tilde{b}_1,\ H\tilde{b}_1,\ A\tilde{b}_1. \tag{13.11b}$$

Unlike squarks of the first two generations, both light and heavy bottom squarks can potentially decay to charginos and W bosons, since they are mixtures of left- and

[5] For yet larger values of $m_{1/2}$ gluino decays to t-quarks are kinematically unsuppressed, and these serve as an additional source of b-jets.

https://doi.org/10.1017/9781009289801.014 Published online by Cambridge University Press

right-squarks. Likewise, top squarks can decay via

$$\tilde{t}_{1,2} \to t\tilde{g},\ t\widetilde{Z}_i,\ b\widetilde{W}_j,\ W\tilde{b}_{1,2},\ H^+\tilde{b}_{1,2} \quad \text{and} \tag{13.12a}$$

$$\tilde{t}_2 \to Z\tilde{t}_1,\ h\tilde{t}_1,\ H\tilde{t}_1,\ A\tilde{t}_1. \tag{13.12b}$$

If top squarks are relatively light, they dominantly decay via $\tilde{t}_1 \to b\widetilde{W}_1$, and possibly also via $\tilde{t}_1 \to t\widetilde{Z}_1$. If both these modes are kinematically forbidden, then the $\tilde{t}_1$ can decay via usually suppressed modes

$$\tilde{t}_1 \to c\widetilde{Z}_1,\ b\nu\tilde{\ell}_{\rm L},\ b\ell\tilde{\nu}_{\rm L},\ bW\widetilde{Z}_1, \text{ or } \quad bf\bar{f}'\widetilde{Z}_1, \tag{13.13}$$

where f and $\bar{f}'$ are light SM fermions that couple to the W boson. The first of these decay modes can take place via the off-diagonal terms in the SUSY Lagrangian that give rise to flavor-violating interactions. Even if tree-level flavor-violating interactions are absent in the Lagrangian renormalized at high energy scales, radiative corrections can induce these at the weak scale, giving rise to the flavor-violating decay mode. We assume here that the decay $\tilde{t}_1 \to c\tilde{g}$ (which would be similarly induced) is kinematically forbidden. In models with universal squark masses at the high scale, it has been shown that the decay $\tilde{t}_1 \to c\widetilde{Z}_1$ frequently dominates the four-body decay for rather light top squarks.[6] There are, however, regions of parameter space where the three- and even four-body decay modes can compete with, or even dominate, the $\tilde{t}_1 \to c\widetilde{Z}_1$ decay.

In Fig. 13.6, we show the branching fractions for $\tilde{u}_{\rm L}$ in the MSSM, for fixed values of $\mu = 200\,\text{GeV}$, $m_{\tilde{g}} = 1000\,\text{GeV}$, and $\tan\beta = 5$, versus $m_{\tilde{u}_{\rm L}}$. Gaugino mass unification is also assumed. At a very low value of $m_{\tilde{u}_{\rm L}}$, only the decay $\tilde{u}_{\rm L} \to u\widetilde{Z}_1$ is open, and hence dominates the branching fraction. As $m_{\tilde{u}_{\rm L}}$ increases, new decay modes become accessible. In particular, when $\tilde{u}_{\rm L} \to d\widetilde{W}_1$ becomes accessible, it soon becomes dominant.[7] As $m_{\tilde{u}_{\rm L}}$ increases even further, decays to the heavier charginos and neutralinos become kinematically accessible. Ultimately, decays to the $SU(2)_{\rm L}$ gaugino-like $\widetilde{W}_2$ and $\widetilde{Z}_4$ dominate while decays to the higgsino-like $\widetilde{Z}_3$ are dynamically suppressed. The heavy charginos and neutralinos will subsequently decay as described below so that heavy squarks, like heavy gluinos, will decay via a multi-step cascade that terminates in the LSP. Finally, at very high values of $m_{\tilde{u}_{\rm L}}$, the decay to $u\tilde{g}$ becomes possible, and soon dominates the electroweak decays to charginos and neutralinos. Branching fractions for $\tilde{d}_{\rm L}$ decays shown in Fig. 13.7 are qualitatively similar, except that the $\tilde{d}_{\rm L} \to d\widetilde{Z}_1$ decay is not as rapidly suppressed when other channels open up. Indeed the extremely rapid suppression of $\tilde{u}_{\rm L} \to u\widetilde{Z}_1$

[6] K. Hikasa and M. Kobayashi, *Phys. Rev.* **D36**, 724 (1987).

[7] To understand the branching fractions we note that, in this case, the neutralinos are fairly mixed with $\widetilde{Z}_1$ dominantly bino-like, $\widetilde{Z}_2$ equally mixed in all four components, $\widetilde{Z}_3$ being essentially a higgsino, and $\widetilde{Z}_4$ dominantly wino-like. The two charginos are substantial mixtures of gauginos and higgsinos, with $\widetilde{W}_2$ being the more gaugino-like because $M_2 > \mu$.

https://doi.org/10.1017/9781009289801.014 Published online by Cambridge University Press

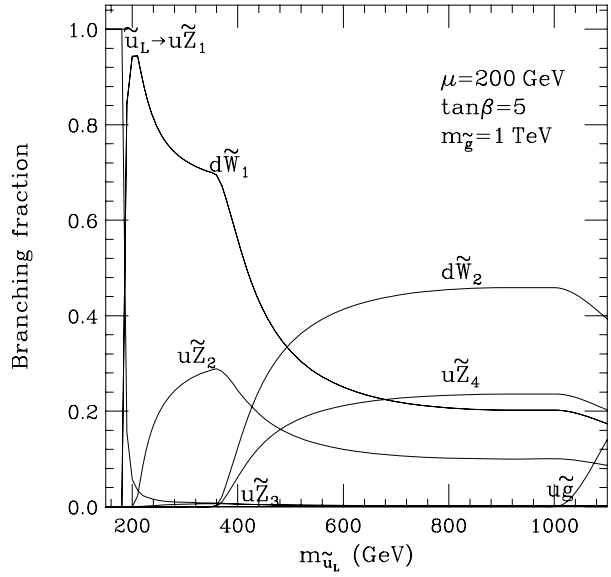

Figure 13.6 Branching fractions of the $\tilde{u}_L$ versus $m_{\tilde{u}_L}$ in the MSSM, assuming gaugino mass unification.

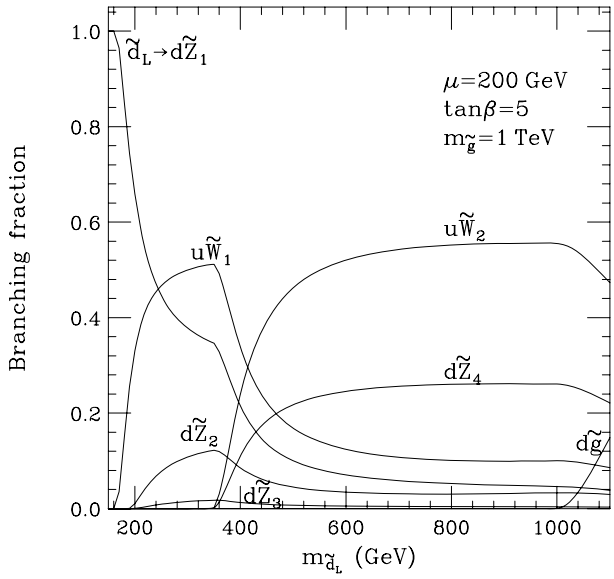

Figure 13.7 Branching fractions of the $\tilde{d}_L$ versus $m_{\tilde{d}_L}$ in the MSSM, assuming gaugino mass unification.

https://doi.org/10.1017/9781009289801.014 Published online by Cambridge University Press

decays in Fig. 13.6 may be attributed to a somewhat accidental cancellation in the corresponding coupling.

In Fig. 13.8 and Fig. 13.9, we show branching fractions of the $\tilde{u}_R$ and $\tilde{d}_R$ squarks in the MSSM model versus the corresponding squark mass, for the same parameters as in Fig. 13.6. Since right-handed squarks are $SU(2)_L$ singlets, these can only decay to neutralinos, and (neglecting Yukawa couplings) only via their hypercharge gaugino components. The partial widths are, therefore, in the ratio of the corresponding $|v_4^{(i)}|^2$ for both types of squarks. Finally, for very high masses, the decay mode $\tilde{q}_R \to q\tilde{g}$ opens up, and soon dominates the branching fractions.

Exercise *Notice that the form of three boson couplings in Chapter 8 implies that the decays $\tilde{t}_2 \to \tilde{t}_1 Z$, $\tilde{t}_2 \to \tilde{b}_1 W$, and also $\tilde{t}_i \to \tilde{b}_j H^+$ (and the corresponding sbottom decays) may occur via gauge interactions. This would suggest that these decays may be relevant also for the first two generations of squarks. Verify that if Yukawa couplings can be ignored, the relevant coupling to Z vanishes, and further, that the decays of $\tilde{d}_L$ to W and $H^\pm$ bosons are kinematically forbidden assuming that $m_{\tilde{u}_L} + m_{\tilde{d}_L} > M_W$. Convince yourself that two-body decays to h, H, and A can only occur via Yukawa couplings.*

13.3 Slepton decays

First generation sleptons may decay via the following two-body modes, if kinematically allowed:

$$\tilde{e}_L \to e\widetilde{Z}_i,\ \nu_e\widetilde{W}_j^-, \tag{13.14a}$$

$$\tilde{\nu}_e \to \nu_e\widetilde{Z}_i,\ e\widetilde{W}_j^+, \tag{13.14b}$$

$$\tilde{e}_R \to e\widetilde{Z}_i. \tag{13.14c}$$

Decays to W, Z and Higgs bosons are not possible for the same reasons as for first generation squarks. Smuons and muon sneutrinos have identical decay patterns and branching fractions as their first generation cousins. The partial widths for these decays are given by (B.53a)–(B.54b) of Appendix B.

We illustrate the branching fractions of the left-selectron, the right-selectron, and the sneutrino in Fig. 13.10, Fig. 13.11, and Fig. 13.12, respectively, as a function of the corresponding sparticle mass for the same MSSM parameters as Fig. 13.6. Except for the fact that these sleptons and sneutrinos never have two-body decays to gluinos, the decay patterns are qualitatively very similar to those of the corresponding squarks that we examined in the last section. In particular, while very light $SU(2)_L$ doublet sleptons $\tilde{e}_L$ and $\tilde{\nu}_e$ can only decay to the LSP, the branching

https://doi.org/10.1017/9781009289801.014 Published online by Cambridge University Press

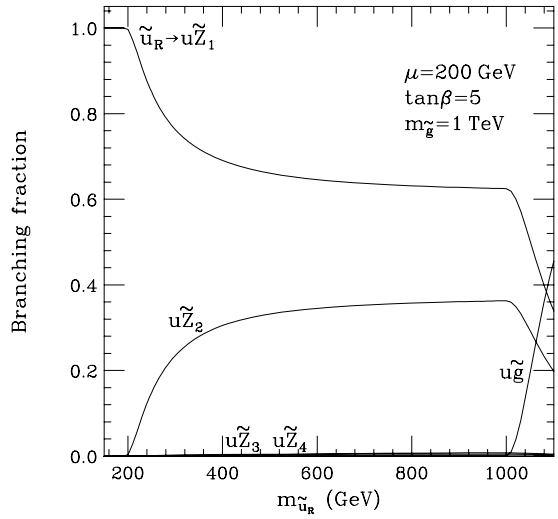

Figure 13.8 Branching fractions of the $\tilde{u}_R$ versus $m_{\tilde{u}_R}$ in the MSSM, assuming gaugino mass unification.

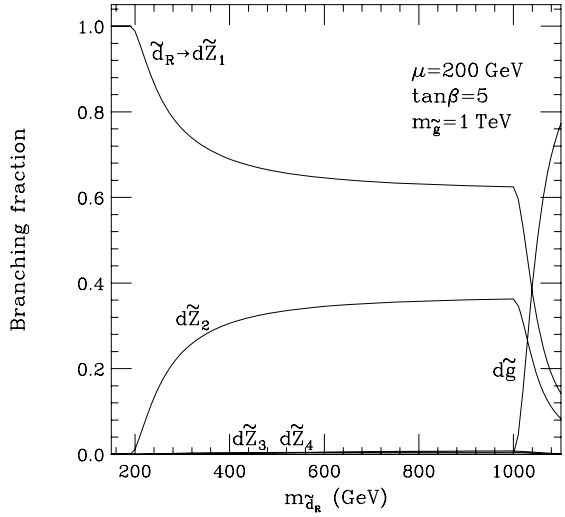

Figure 13.9 Branching fractions of the $\tilde{d}_R$ versus $m_{\tilde{d}_R}$ in the MSSM, assuming gaugino mass unification.

fractions for their decays to heavier charginos and neutralinos become dominant if these decays are not kinematically suppressed.[8] Thus a sneutrino heavier than the chargino is expected to have a significant branching fraction for visible decays.

[8] The strong suppression of the $\tilde{\nu}_e \to \widetilde{Z}_2 \nu$ decay is accidental.

https://doi.org/10.1017/9781009289801.014 Published online by Cambridge University Press

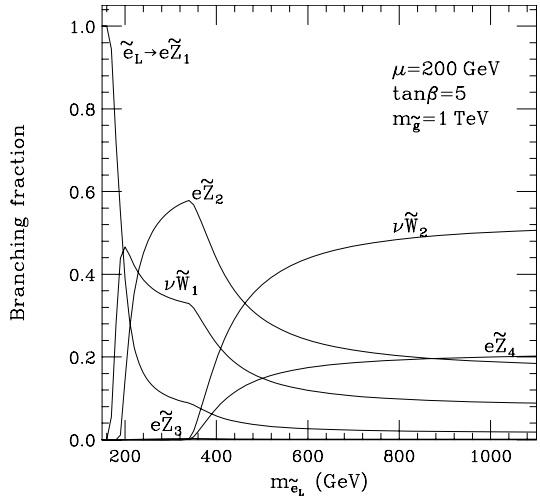

Figure 13.10 Branching fractions of the $\tilde{e}_L$ versus $m_{\tilde{e}_L}$ in the MSSM, assuming gaugino mass unification.

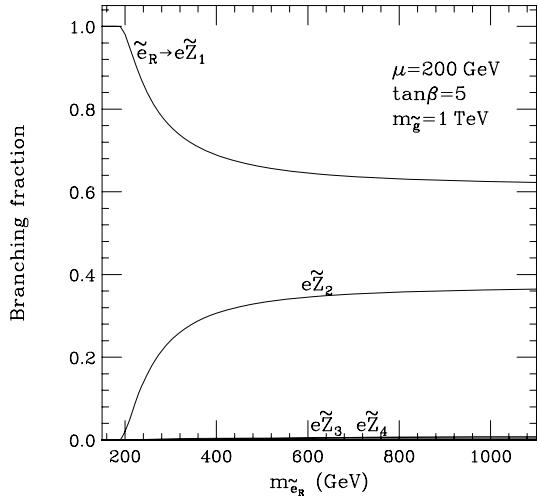

Figure 13.11 Branching fractions of the $\tilde{e}_R$ versus $m_{\tilde{e}_R}$ in the MSSM, assuming gaugino mass unification.

The right-selectron, like its squark cousin $\tilde{d}_R$, can only decay to neutralinos via the hypercharge gauge coupling: since $\widetilde{Z}_1$ has the largest bino component, this decay always dominates. As a result, $\tilde{\ell}_R$ pair production leads to events with opposite sign/same flavor dilepton pairs plus large missing energy.

Just as with third generation squarks, the decay possibilities of third generation sleptons are more complicated due to Yukawa coupling and mixing effects. The

https://doi.org/10.1017/9781009289801.014 Published online by Cambridge University Press

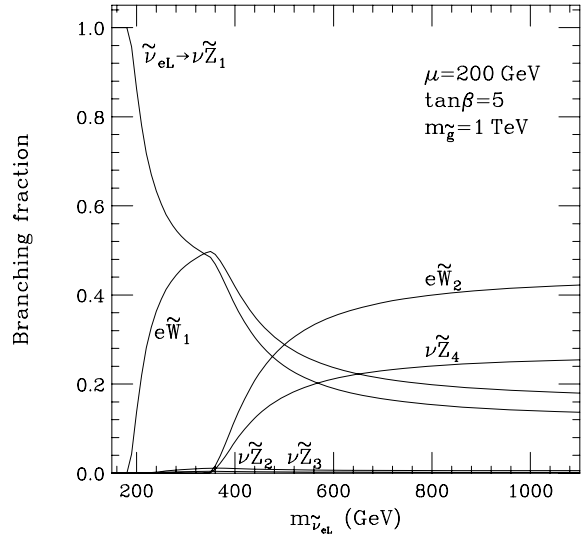

Figure 13.12 Branching fractions of the $\tilde{\nu}_{eL}$ versus $m_{\tilde{\nu}_{eL}}$ in the MSSM, assuming gaugino mass unification.

decay possibilities, not all of which may be kinematically allowed, include

$$\tilde{\tau}_1 \to \tau \widetilde{Z}_i,\ \nu_\tau \widetilde{W}_j, \tag{13.15a}$$

$$\tilde{\tau}_2 \to \tau \widetilde{Z}_i,\ \nu_\tau \widetilde{W}_j,\ W\tilde{\nu}_\tau,\ H^-\tilde{\nu}_\tau, \tag{13.15b}$$

$$\tilde{\tau}_2 \to Z\tilde{\tau}_1,\ h\tilde{\tau}_1,\ H\tilde{\tau}_1,\ A\tilde{\tau}_1, \tag{13.15c}$$

$$\tilde{\nu}_\tau \to \nu_\tau \widetilde{Z}_i,\ \tau \widetilde{W}_j,\ W\tilde{\tau}_{1,2} \quad \text{and} \quad H^+\tilde{\tau}_{1,2}. \tag{13.15d}$$

The partial widths for these decays may be found in Appendix B.3.

In gauge-mediated SUSY breaking models with a low scale of SUSY breaking and a light gravitino, the $\tilde{\tau}_1$ slepton may be the next-to-lightest SUSY particle (NLSP), while the gravitino $\tilde{G}$ is the LSP. In this case, $\widetilde{Z}_1$ may be heavier than some of the sleptons. The right-handed sleptons of the first two generations (these would be much lighter than their left-handed sisters) would then dominantly decay via

$$\tilde{\ell}_R \to \tilde{\tau}_1^- \tau^+ \ell \text{ and } \tilde{\ell}_R \to \tilde{\tau}_1^+ \tau^- \ell \tag{13.16a}$$

mediated by neutralino exchange (recall that these couple to charginos only via tiny Yukawa couplings) which usually dominates the two-body decay $\tilde{\ell}_R \to \ell\tilde{G}$ (even for $C_{\rm grav} = 1$) as long as these are not strongly suppressed by kinematics. For the case of the "co-NLSP" scenario where the sleptons of all three generations are almost degenerate, and $m_{\tilde{\ell}_1} - m_{\tilde{\tau}_1} < m_\tau$, the decay $\tilde{\ell}_1 \to \ell\tilde{G}$ dominates if $C_{\rm grav} = 1$;

https://doi.org/10.1017/9781009289801.014 Published online by Cambridge University Press

for larger values of $C_{\rm grav}$, the decay

$$\tilde{\mu}_1 \to \tilde{\tau}_1 \bar{\nu}_\tau \nu_\mu \tag{13.16b}$$

mediated by muon Yukawa couplings to a virtual chargino can potentially compete with the decay to the gravitino. In this case, the lifetimes of the NLSP may be large, and there may be displaced vertices or detectable charged sparticle tracks in the experimental apparatus.[9]

13.4 Chargino decays

Charginos decay only via electroweak interactions. They would dominantly decay via the following two-body modes if these are kinematically unsuppressed:

$$\widetilde{W}_j \to W\widetilde{Z}_i,\ H^-\widetilde{Z}_i, \tag{13.17a}$$

$$\to \tilde{u}_{\rm L}\bar{d},\ \bar{\tilde{d}}_{\rm L}u,\ \tilde{c}_{\rm L}\bar{s},\ \bar{\tilde{s}}_{\rm L}c,\ \tilde{t}_{1,2}\bar{b},\ \tilde{b}_{1,2}t, \tag{13.17b}$$

$$\to \tilde{\nu}_e\bar{e},\ \bar{\tilde{e}}_{\rm L}\nu_e,\ \tilde{\nu}_\mu\bar{\mu},\ \bar{\tilde{\mu}}_{\rm L}\nu_\mu,\ \tilde{\nu}_\tau\bar{\tau},\bar{\tilde{\tau}}_{1,2}\nu_\tau,\ \text{and} \tag{13.17c}$$

$$\widetilde{W}_2 \to Z\widetilde{W}_1,\ h\widetilde{W}_1,\ H\widetilde{W}_1,\ \text{and}\ A\widetilde{W}_1. \tag{13.17d}$$

Partial widths for these decays are listed in Appendix B.5.1.

If all these modes are suppressed or forbidden (as may be the case for charginos in the mass range accessible to Tevatron searches), then three-body modes mediated by virtual bosons will dominate. Charginos may decay to a lighter neutralino via

$$\widetilde{W}_j \to \widetilde{Z}_i + f\bar{f}', \tag{13.18a}$$

where f and $\bar{f}'$ are light SM fermions that couple to the W boson. For the lighter chargino, usually only the three-body decays to the $\widetilde{Z}_1$ are relevant. The heavy chargino may also decay via

$$\widetilde{W}_2 \to \widetilde{W}_1 f\bar{f} \tag{13.18b}$$

as well.

Feynman diagrams for leading order contributions to $\widetilde{W}_1 \to e\bar{\nu}_e\widetilde{Z}_1$ decay are shown in Fig. 13.13. Three-body decays to other leptons or to quarks occur via analogous diagrams. For decays to the first two generations of fermions, Yukawa couplings, and hence also intragenerational sfermion mixings, are small; thus $\tilde{e}_{\rm R}$ and H^+ exchange diagrams make negligible contributions. However, for $\widetilde{W}_1 \to \tau\bar{\nu}_\tau\widetilde{Z}_1$ decay, these contributions can be important if $\tan\beta$ is large. The partial width for the decay $\widetilde{W}_1 \to \tau\tilde{\nu}_\tau\widetilde{Z}_1$ is given in Appendix B.5.2. The corresponding widths for

[9] For a discussion of three-body decays of sleptons, see S. Ambrosanio, G. Kribs and S. Martin, *Nucl. Phys.* **B516**, 55 (1998) and H. Baer, P. Mercadante, X. Tata and Y. Wang, *Phys. Rev.* **D60**, 055001 (1999).

https://doi.org/10.1017/9781009289801.014 Published online by Cambridge University Press

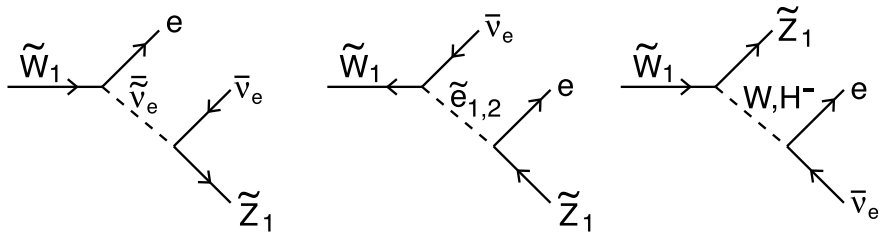

Figure 13.13 Feynman diagrams contributing to the decay $\widetilde{W}_1 \to e\bar{\nu}_e\widetilde{Z}_1$.

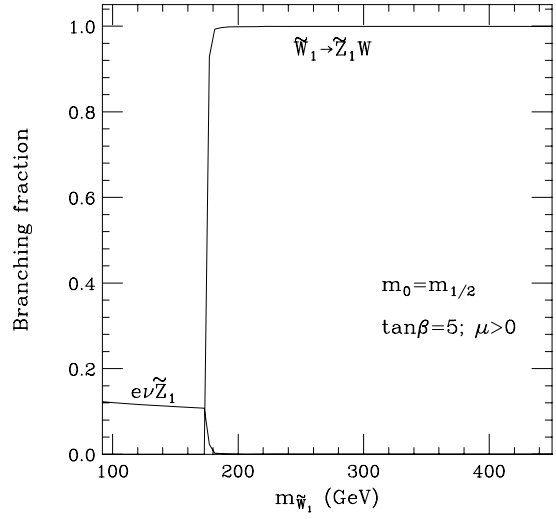

Figure 13.14 Branching fractions for decays of $\widetilde{W}_1$ versus $m_{\widetilde{W}_1}$ in the mSUGRA model. Below the threshold for $\widetilde{W}_1 \to W\widetilde{Z}_1$ decay, decays to other leptons families have essentially the same branching ratio as that for $\widetilde{W}_1 e\nu$. The rest of the time the chargino decays hadronically with these decays distributed essentially equally between the first two generations.

other decays can be obtained from this by setting the Yukawa coupling and the tau lepton mass to zero, and including appropriate color factors as spelled out there.

We illustrate the $\widetilde{W}_1$ decay branching ratio in Fig. 13.14 versus $m_{\widetilde{W}_1}$ for the mSUGRA model with parameters $m_0 = m_{1/2}$, $\tan\beta = 5$, $A_0 = 0$, and $\mu > 0$. In this case, squarks are much heavier than M_W and, except for the lowest values of the chargino mass, so are sleptons and sneutrinos. For $m_{\widetilde{W}_1} < M_W + m_{\widetilde{Z}_1}$ the amplitude for the decay is dominated by the virtual W boson exchange, resulting in a branching ratio $B(\widetilde{W}_1 \to \widetilde{Z}_1 f\bar{f}') \simeq B(W \to f\bar{f}')$, which is close to 11% for the decay $\widetilde{W}_1 \to \widetilde{Z}_1 e\nu$; the small increase in this branching for very low $m_{\widetilde{W}_1}$ values is due to contributions from slepton and sneutrino exchanges. Here, it is worth recalling the relative robustness of the $W\widetilde{W}_1\widetilde{Z}_1$ coupling that we mentioned below

https://doi.org/10.1017/9781009289801.014 Published online by Cambridge University Press

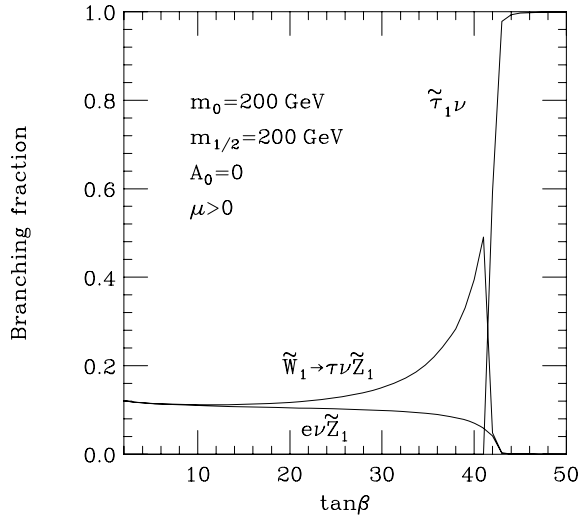

Figure 13.15 Branching fractions of the $\widetilde{W}_1$ versus $\tan\beta$ in the mSUGRA model with parameters as shown in the figure.

(8.103b): since this coupling is usually unsuppressed, the W exchange contribution tends to dominate chargino three-body decays if sfermions are heavy and $\tan\beta$ is not very large, so that chargino branching fractions to $\widetilde{Z}_1 f \bar{f}'$ are frequently close to those for $W \to f\bar{f}'$ decays. As $m_{\widetilde{W}_1}$ increases, the two-body mode $\widetilde{W}_1 \to W\widetilde{Z}_1$ opens up, and quickly dominates the branching fraction. The final state particles of the $\widetilde{W}_1$ decay (and the branching ratios) are the same as for low $m_{\widetilde{W}_1}$ values, but now the W boson is real instead of virtual.

The $\tan\beta$ dependence of the branching fractions of $\widetilde{W}_1$ is illustrated in Fig. 13.15 for the same mSUGRA model parameters as in the previous figure, but with $m_0 = m_{1/2} = 200$ GeV. For low values of $\tan\beta$, the chargino dominantly decays via $\widetilde{W}_1 \to f\bar{f}'\widetilde{Z}_1$ with branching fractions equal to those for $W \to f\bar{f}'$ as for the case of Fig. 13.14. As $\tan\beta$ increases, the τ Yukawa coupling grows, and the $\tilde{\tau}_1$ mass decreases due to Yukawa coupling contributions to RGE running, and due to non-negligible mixing effects. For $\tan\beta \sim 15$, the two branching fractions begin to separate and decays to τs become increasingly important; for large values of $\tan\beta$, contributions from the higgsino component of the chargino may also be relevant. The decay amplitude from the virtual $\tilde{\tau}_1$ Feynman diagram becomes comparable to and even larger than the virtual W contribution. For very large values of $\tan\beta$, the $\tilde{\tau}_1$ becomes so light that $\widetilde{W}_1 \to \tilde{\tau}_1 \nu_\tau$ becomes accessible, and quickly dominates the branching fraction even though $\tilde{\tau}_1$ is dominantly $\tilde{\tau}_R$.

Heavy charginos usually decay via two-body modes. Their decay patterns are highly model and parameter-space dependent. The decay products of $\widetilde{W}_2$ frequently include W, Z, and Higgs bosons, and sometimes also sleptons. Indeed if $\widetilde{W}_2$s are

https://doi.org/10.1017/9781009289801.014 Published online by Cambridge University Press

produced via cascade decays of heavy sparticles, very rich phenomenology results. We refer the reader to the literature for a discussion and illustrative examples of the branching ratios of $\widetilde{W}_2$.[10]

13.4.1 A chargino degenerate with the LSP

Within the MSSM, it is possible that $m_{\widetilde{W}_1} \simeq m_{\widetilde{Z}_1}$ if either $|M_1|, |M_2| \gg |\mu|, M_W$ or $|M_1|, |\mu| \gg |M_2|, |M_W|$. In the first case, the light chargino and the lightest two neutralinos are higgsino-like with masses close to $|\mu|$. Any splitting between the chargino and the $\widetilde{Z}_1$ mass has to be an $SU(2)_{\rm L}$ breaking effect, i.e. it has to come from mixing between the gauginos and higgsinos. It is not difficult to show (see exercise below) that the splitting is $\mathcal{O}(M_W^2/\Lambda)$, where $\Lambda \sim |M_1|$ or $|M_2|$ is the large scale in the chargino and neutralino mass matrices. For an $SU(2)_{\rm L}$ gaugino mass an order of magnitude larger than M_W, a mass splitting of $\mathcal{O}(10)$ GeV may be expected. This small mass gap implies that the visible products from chargino decay will be rather soft compared to expectations in mSUGRA or mGMSB models, but the decay patterns of the charginos are qualitatively similar to those we have just discussed.[11]

In the second case where $|M_1|, |\mu| \gg |M_2|, M_W$, the $SU(2)_{\rm L}$ gaugino would be lighter than the higgsinos or the hypercharge gauginos and in the absence of any gaugino–higgsino mixing we would expect that $\widetilde{Z}_1$ and $\widetilde{W}_1^{\pm}$ form a weak isotriplet with a mass $|M_2|$. The degeneracy again should not be surprising because any mass splitting between the charged and neutral winos has to be an $SU(2)_{\rm L}$ breaking effect and, at tree level, gaugino–higgsino mixing is the only source of $SU(2)_{\rm L}$ breaking. It is tedious but straightforward to show that in this case the tree-level mass splitting between the chargino and neutralino is $\mathcal{O}(M_W^4/\Lambda^3)$ where $\Lambda \sim |M_1|$ or $|\mu|$ is the large scale in the mass matrices. For an order of magnitude hierarchy between M_W and Λ, this corresponds to a sub-GeV mass gap. Then, the contribution to the mass splitting from radiative corrections can potentially be comparable to or even much larger than the tree-level splitting. These corrections have been evaluated,[12] and it has been shown that radiative corrections make the dominant contribution to the mass gap within the minimal anomaly-mediated SUSY breaking (AMSB) model which provides an example of just such a chargino–neutralino spectrum. Detailed calculation shows that the chargino–neutralino mass gap is typically 160–250 MeV. Fortunately, $m_{\widetilde{W}_1} > m_{\widetilde{Z}_1}$ so that the LSP is still neutral.

[10] See, e.g., H. Baer, A. Bartl, D. Karatas, W. Majerotto and X. Tata, *Int. J. Mod. Phys.* **A4**, 4111 (1989).
[11] Although $|\mu|$ is generically large within the mSUGRA framework, the recent determination of the relic dark matter density by the WMAP collaboration prefers selected regions of mSUGRA parameter space: in one of these regions, dubbed the hyperbolic branch region, $|\mu|$ may be much smaller than the gaugino masses.
[12] See e.g. D. Pierce and A. Papadopoulos, *Nucl. Phys.* **B430**, 278 (1994).

https://doi.org/10.1017/9781009289801.014 Published online by Cambridge University Press

For such a small splitting, chargino decays are qualitatively altered from our discussion above. If $m_{\widetilde{W}_1} - m_{\widetilde{Z}_1} < m_\pi$, hadronic decays of the chargino are kinematically forbidden, and the chargino would dominantly decay via $\widetilde{W}_1^- \to e\nu\widetilde{Z}_1$, the mode with the largest phase space. The chargino could be rather long lived and could traverse a considerable distance before decaying, so there would be a charged particle track with a kink in the detector. If the decay $\widetilde{W}_1^- \to \pi^-\widetilde{Z}_1$ is allowed, the chargino decay length would be only a few centimeters, and the chargino track would then be more difficult to identify. For yet larger mass gaps, multi-pion decays would become possible and the lifetime would be even shorter.[13]

Exercise *For the case where the magnitude of the gaugino masses is much larger than $|\mu|$ or M_W, show that the eigenvalues of the neutralino mass matrix shift by:*

$$\mu \to \mu + \frac{1}{2}M_W^2(1 - \sin 2\beta)\left[\frac{1}{M_2} + \frac{\tan^2\theta_W}{M_1}\right], \tag{13.19a}$$

$$-\mu \to -\mu + \frac{1}{2}M_W^2(1 + \sin 2\beta)\left[\frac{1}{M_2} + \frac{\tan^2\theta_W}{M_1}\right], \tag{13.19b}$$

while the chargino mass (for $\mu > 0$) is given by,

$$m_{\widetilde{W}_1} = \mu + \frac{M_W^2}{M_2}\sin 2\beta. \tag{13.19c}$$

Hint: To find the shift of the neutralino eigenvalues, write the neutralino mass matrix in the basis where the higgsino sub-matrix is diagonal, and then treat the off-diagonal entries of the neutralino mass matrix in the new basis using standard second order perturbation theory. The chargino mass may be obtained using (8.54).

13.5 Neutralino decays

Like charginos, neutralinos dominantly decay via the following two-body modes if these are kinematically accessible:

$$\widetilde{Z}_i \to W\widetilde{W}_j,\ H^+\widetilde{W}_j,\ Z\widetilde{Z}_{i'},\ h\widetilde{Z}_{i'},\ H\widetilde{Z}_{i'},\ A\widetilde{Z}_{i'} \tag{13.20a}$$

$$\to \tilde{q}_{\mathrm{L,R}}\bar{q},\ \overline{\tilde{q}}_{\mathrm{L,R}}q,\ \tilde{\ell}_{\mathrm{L,R}}\bar{\ell},\ \overline{\tilde{\ell}}_{\mathrm{L,R}}\ell,\ \tilde{\nu}_\ell\bar{\nu}_\ell,\ \bar{\tilde{\nu}}_\ell\nu_\ell. \tag{13.20b}$$

Here, $i, i' = 1$–4 with $i > i'$, and q and ℓ denote all possible quark and lepton flavors. The partial widths for these decays are listed in Appendix B.4.1.

[13] Formulae for $\widetilde{W}_1$ decay for a tiny $m_{\widetilde{W}_1} - m_{\widetilde{Z}_1}$ mass difference can be found in C. H. Chen, M. Drees and J. F. Gunion, *Phys. Rev.* **D55**, 330 (1997), (erratum-ibid. **60**, 039901,1999).

https://doi.org/10.1017/9781009289801.014 Published online by Cambridge University Press

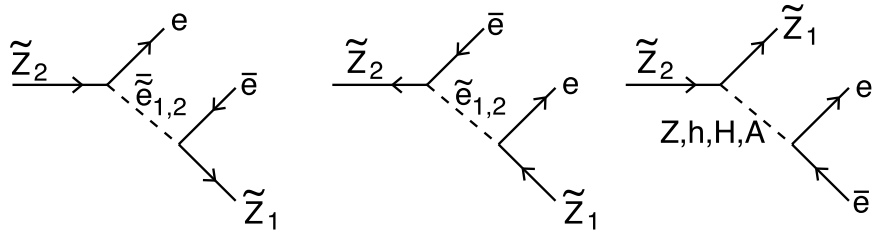

Figure 13.16 Feynman diagrams contributing to the decay $\widetilde{Z}_2 \to e\bar{e}\widetilde{Z}_1$.

If all these two-body modes are suppressed or kinematically forbidden, then the neutralino usually decays via

$$\widetilde{Z}_i \to \widetilde{Z}_{i'} + f\,\bar{f} \tag{13.21a}$$

where f is a SM quark or lepton. The leading Feynman diagrams contributing to $\widetilde{Z}_2 \to e\bar{e}\widetilde{Z}_1$ decay at leading order are shown in Fig. 13.16, where $\tilde{e}_1$ and $\tilde{e}_2$ are selectron mass eigenstates (that essentially coincide with $\tilde{e}_R$ and $\tilde{e}_L$). Decays to other fermion flavors in (13.21a) as well as of other neutralinos occur via analogous diagrams. For decays to the first two generations, the three diagrams involving the Higgs bosons make a negligible contribution. The partial width for this decay is given in B.4.2. In addition, the three-body mode

$$\widetilde{Z}_i \to \widetilde{W}_j + f\,\bar{f}', \tag{13.21b}$$

which occurs via diagrams analogous to those in Fig. 13.13 may also be relevant. Its partial width is given by Eq. (B.106) of Appendix B.

Neutralinos can also decay via

$$\widetilde{Z}_i \to \gamma\,\widetilde{Z}_{i'} \tag{13.22}$$

at the one-loop level via diagrams involving charged sfermions/fermions and charginos/W or charged Higgs bosons in the loop. The branching fraction for this decay is usually small. However, it can be important if the widths of three-body modes are somehow suppressed. This suppression may occur either if one of the neutralinos is photino-like and the other higgsino-like since the photino (higgsino) does not couple to the Z boson (sfermion), or if both neutralinos are very close in mass because the strong three-body phase space suppression favors two-body decays. We do not list the partial width for this decay but will refer the interested reader to the original literature for this computation.[14]

[14] H. E. Haber and D. Wyler, *Nucl. Phys.* **B323**, 267 (1989); see also H. Baer and T. Krupovnickas, *JHEP* **0209**, 038 (2002).

https://doi.org/10.1017/9781009289801.014 Published online by Cambridge University Press

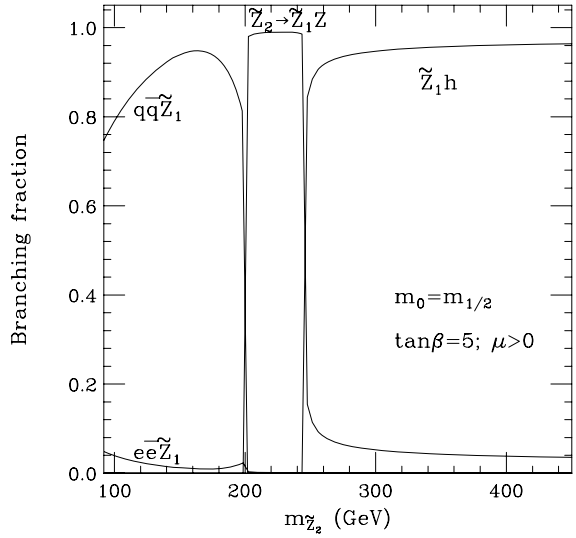

Figure 13.17 Branching fractions of the $\widetilde{Z}_2$ versus $m_{\widetilde{Z}_2}$ in the mSUGRA model. The branching ratios are almost generation independent for this low value of $\tan\beta$. The hadronic decays are summed over all quark flavors. Invisible decays make up the remainder of the branching fraction at low values of $m_{\widetilde{Z}_1}$.

Since $\widetilde{Z}_2$ is likely to be the most accessible visibly decaying neutralino, we show the branching fractions for its various decays in Fig. 13.17, assuming the mSUGRA model framework, and for the same model parameters as in Fig. 13.14. For low values of $m_{\widetilde{Z}_2}$, the two-body decay modes are all inaccessible, and $\widetilde{Z}_2$ mainly decays via three-body modes. If we compare these branching fractions to those for chargino decay in Fig. 13.14, we are immediately struck by the fact that while the branching fractions for chargino three-body decays were close to those for the W boson, the branching fractions for the neutralino decay $\widetilde{Z}_2 \to \widetilde{Z}_1 f \bar{f}$ differ considerably from those of $Z \to f\bar{f}$: i.e. even for sfermions considerably heavier than M_Z, the Z exchange graph does not dominate. This is because the couplings of Z to neutralinos are very sensitive to model parameters and, as we have discussed below (8.101), can be considerably suppressed. When this occurs, slepton exchange amplitudes remain important even for slepton masses of several hundred GeV. Over considerable regions of the MSSM parameter space, the leptonic three-body decays of $\widetilde{Z}_2$ can be either enhanced or suppressed due to interference between scalar and Z boson exchange graphs, and neutralino branching fractions are quite different from those of the Z boson.[15] Neutralino decay patterns (and resulting signatures) are, therefore, much more sensitive to model parameters than those for chargino decays.

[15] For more details, see H. Baer and X. Tata, *Phys. Rev.* **D47**, 2739 (1993).

https://doi.org/10.1017/9781009289801.014 Published online by Cambridge University Press

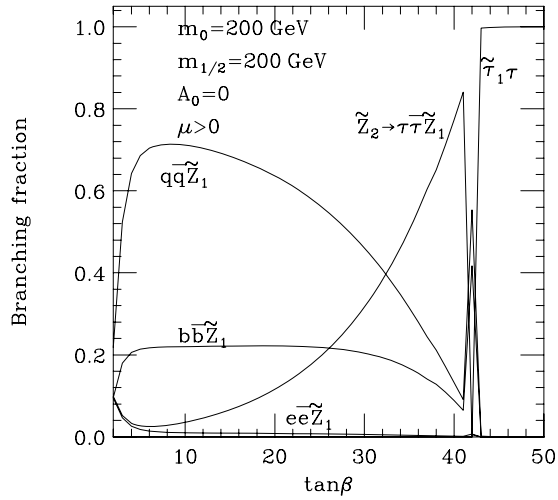

Figure 13.18 Branching fractions of the $\widetilde{Z}_2$ versus $\tan\beta$ in the mSUGRA model. Here $q = u, d, s, c$.

In Fig. 13.17, as $m_{\widetilde{Z}_2}$ increases, ultimately the two-body mode $\widetilde{Z}_2 \to Z\widetilde{Z}_1$ becomes accessible, and dominant. At even higher values of $m_{\widetilde{Z}_2}$, the decay mode $\widetilde{Z}_2 \to h\widetilde{Z}_1$ becomes accessible, and in this case quickly dominates. In SUSY particle cascade decays, we may expect an assortment of Higgs and vector bosons to be present.

In Fig. 13.18, we again show $\widetilde{Z}_2$ decay branching fractions in the mSUGRA model, but this time versus $\tan\beta$ and for the same parameters as in Fig. 13.15. At very low $\tan\beta$, $\widetilde{Z}_2$ decays via three-body modes with a large branching fraction into charged leptons. Decays into first, second, and third generation charged leptons occur at nearly the same rate. As $\tan\beta$ increases, the leptonic branching fraction drops and decays to quarks become increasingly dominant. The branching fraction into tau pairs begins diverging from that to electron (and muon) pairs around $\tan\beta \sim 5$. The decays to bottom quarks become more important relative to other hadronic decays but, in this example, decay to $\tau\bar{\tau}\widetilde{Z}_1$ becomes dominant for $\tan\beta \sim 30$, due to the enhanced tau lepton Yukawa coupling, and the gradual suppression of $m_{\tilde{\tau}_1}$. Finally, around $\tan\beta \gtrsim 42$, two-body decays to $\tilde{\tau}_1\bar{\tau}$ and $\bar{\tilde{\tau}}_1\tau$ turn on, and quickly dominate the branching fraction.

13.6 Decays of the Higgs bosons

Both the neutral and charged physical spin zero particles associated with the electroweak symmetry breaking sector dominantly decay via two-body modes into SM particles or, if they are heavy enough, also into lighter SUSY particles. The partial widths for the dominant tree level decays of Higgs bosons are listed in Appendix C.

https://doi.org/10.1017/9781009289801.014 Published online by Cambridge University Press

13.6.1 Light scalar h

At tree level, the light scalar Higgs boson h can decay via the two-body modes,

$$h \to u\bar{u},\ d\bar{d},\ s\bar{s},\ c\bar{c},\ b\bar{b},\ e\bar{e},\ \mu\bar{\mu},\ \tau\bar{\tau}, \tag{13.23a}$$

$$h \to \widetilde{Z}_i \widetilde{Z}_{i'},\ \widetilde{W}_j^+ \widetilde{W}_{j'}^-,\ \tilde{f}\bar{\tilde{f}}, \tag{13.23b}$$

$$h \to AA \tag{13.23c}$$

where $i, i' = 1$–4 and $j, j' = 1, 2$. Since m_h is expected to be smaller than about 135 GeV within the MSSM framework with perturbative gauge couplings up to the GUT scale, its decays to $t\bar{t}$, W^+W^-, and ZZ are kinematically forbidden. Its decays to SUSY particles, possibly other than $\widetilde{Z}_1\widetilde{Z}_1$, are also expected to be suppressed. Over much of the parameter space, $h \to b\bar{b}$ decays dominate. For small to moderate values of $\tan\beta$, the bottom Yukawa coupling is small, and the h is narrow. In this case, especially the first of the three-body modes

$$h \to Wf\bar{f}'/Zf\bar{f} \tag{13.24}$$

may also be significant, particularly at the upper end of the m_h range. Since the h couples to mass, it dominantly decays to $b\bar{b}$ with a branching fraction of about 85%, and to $\tau\bar{\tau}$ pairs. The ratio of their branching ratios is fixed at tree level, but may be significantly affected by SUSY radiative corrections to the relation between the fermion mass and the corresponding Yukawa coupling. If neutralinos are light enough, h may also decay invisibly to $\widetilde{Z}_1\widetilde{Z}_1$. This decay, which occurs via gauge interactions, can potentially have a large branching fraction, although this is unlikely within constrained frameworks such as mSUGRA because of experimental limits on $m_{\widetilde{Z}_1}$.

Finally, h can also decay via

$$h \to gg,\ \gamma\gamma,\ Z\gamma, \tag{13.25}$$

through loops of gauge/Higgs sector fields and SM fermions, as well as their SUSY counterparts. Although the branching fractions for these decays are always suppressed by coupling and loop factors, the $h \to \gamma\gamma$ decay is an important search mode for LHC experiments which have excellent electromagnetic resolution. The $h \to \gamma\gamma$ branching fraction, which is $\mathcal{O}(10^{-3})$ for a SM-like h in the 100–120 GeV range, is enhanced for some ranges of SUSY parameters.[16]

[16] The h, H, and A can all decay via loop diagrams to $\gamma\gamma$ as well as to gg pairs. Formulae for these partial widths may be found in J. F. Gunion, H. E. Haber, G. Kane and S. Dawson, *The Higgs Hunter's Guide*, Addison-Wesley (1990); M. Bisset, U. of Hawaii thesis, UH-511-813-94 (1994).

https://doi.org/10.1017/9781009289801.014 Published online by Cambridge University Press

13.6.2 Heavy scalar H

The heavy scalar Higgs boson H decays via the two-body modes

$$H \to u\bar{u},\ d\bar{d},\ s\bar{s},\ c\bar{c},\ b\bar{b},\ t\bar{t},\ e\bar{e},\ \mu\bar{\mu},\ \tau\bar{\tau}, \tag{13.26a}$$
$$\to WW,\ ZZ \tag{13.26b}$$
$$\to \widetilde{Z}_i\widetilde{Z}_{i'},\ \widetilde{W}_j^+\widetilde{W}_{j'}^-,\ \tilde{f}\bar{\tilde{f}}, \tag{13.26c}$$
$$\to hh,\ AA,\ H^+H^-,\ AZ, \tag{13.26d}$$
$$\to gg,\ \gamma\gamma,\ Z\gamma, \tag{13.26e}$$

as well as to (usually strongly suppressed) three-body modes, as does the h. If $m_A \gtrsim 200$ GeV, h is essentially a SM Higgs boson, and decays of H to vector bosons are suppressed by a factor $\cos^2(\alpha+\beta)$ (see the exercise below). Hence, the heavy scalar usually decays to $t\bar{t}$, $b\bar{b}$, hh or SUSY particles. As $\tan\beta$ increases, decays to $b\bar{b}$ and $\tau\bar{\tau}$ are enhanced relative to decays to $t\bar{t}$. SUSY decay modes of interest include the invisible $H \to \widetilde{Z}_1\widetilde{Z}_1$ channel, $H \to \widetilde{W}_1\widetilde{W}_1$, and $H \to \widetilde{Z}_2\widetilde{Z}_2$. This last decay results in gold-plated four isolated lepton events with missing energy if both neutralinos decay via $\widetilde{Z}_2 \to \ell\bar{\ell}\widetilde{Z}_1$.

Exercise *Starting from Eq. (8.40b) verify that* $\tan\alpha \to \cot\beta$ *as* $m_A \to \infty$*, so that* $\cos(\alpha+\beta) \to 0$ *in the same limit.*

13.6.3 Pseudoscalar A

The pseudoscalar Higgs boson A can decay via

$$A \to u\bar{u},\ d\bar{d},\ s\bar{s},\ c\bar{c},\ b\bar{b},\ t\bar{t},\ e\bar{e},\ \mu\bar{\mu},\ \tau\bar{\tau}, \tag{13.27a}$$
$$\to \widetilde{Z}_i\widetilde{Z}_{i'},\ \widetilde{W}_j^+\widetilde{W}_{j'}^-,\ \tilde{f}\bar{\tilde{f}}, \tag{13.27b}$$
$$\to hZ, \tag{13.27c}$$
$$\to gg,\ \gamma\gamma. \tag{13.27d}$$

Since A does not couple to vector boson pairs at tree level, its dominant decays are to $t\bar{t}$ or $b\bar{b}$ and $\tau\bar{\tau}$, unless its decays to hZ or SUSY particles are accessible: if this is the case, these latter decays usually dominate.

We remark that if CP is violated in the Higgs sector, A would mix with h and H, and its decay patterns would be qualitatively altered.

https://doi.org/10.1017/9781009289801.014 Published online by Cambridge University Press

13.6.4 Charged scalar $H^{\pm}$

The charged Higgs H^+ dominantly decays via

$$H^+ \to u\bar{d},\ c\bar{s},\ t\bar{b},\ \nu_e\bar{e},\ \nu_\mu\bar{\mu},\ \nu_\tau\bar{\tau}, \tag{13.28a}$$
$$\to \widetilde{Z}_i\widetilde{W}_j^+,\ \tilde{f}\bar{\tilde{f}}', \tag{13.28b}$$
$$\to hW. \tag{13.28c}$$

Notice that, within the MSSM, the decay $H^+ \to W^+Z^0$ is absent at tree level. Thus, it dominantly decays to $t\bar{b}$, unless decays to hW or SUSY particles are open. If $H^+ \to t\bar{b}$ decay is also kinematically forbidden, H^+ preferentially decays via $H^+ \to \tau^+\nu_\tau$. In this case, the daughter tau dominantly has the opposite helicity from taus produced in W boson decays.

13.7 Top quark decays to SUSY particles

The top quark may be heavy enough for it to be able to decay to SUSY particles. However, branching fractions for its SUSY decays cannot be too large, as this would lead to inconsistencies between experimental measurements that agree well with SM predictions of top quark production and decay properties. In addition to its SM decay mode,

$$t \to bW^+, \tag{13.29a}$$

the decays

$$t \to bH^+, \tag{13.29b}$$
$$\to \tilde{t}_{1,2}\widetilde{Z}_i,\quad \tilde{b}_{1,2}\widetilde{W}_j \tag{13.29c}$$

are also possible within the MSSM framework. The decay mode $t \to bH^+$ would then usually be followed by $H^+ \to \nu_\tau\bar{\tau}$, so an enhanced production of τ leptons would occur in top quark production events. If $t \to \tilde{t}_1\widetilde{Z}_1$, followed by $\tilde{t}_1 \to b\widetilde{W}_1 \to bf\bar{f}'\widetilde{Z}_1$, then the visible top quark decay products might be the same as in the SM, but with reduced energies, since some energy is taken by the mass of $\widetilde{Z}_1$. Such a decay chain may be almost excluded if we assume gaugino mass unification, but may be allowed if $|M_1| \ll |M_2|$. Alternatively, if $t \to \tilde{t}_1\widetilde{Z}_1$ is followed by $\tilde{t}_1 \to c\widetilde{Z}_1$, then a top quark decay would lead to a charm jet with an energy sensitively dependent upon $m_{\widetilde{Z}_1}$ and $m_{\tilde{t}_1}$.

https://doi.org/10.1017/9781009289801.014 Published online by Cambridge University Press

13.8 Decays to the gravitino/goldstino

If the gravitino is the LSP, sparticles can decay to it. If these decays proceed only via the usual gravitational coupling (as do the decays to gravitinos with helicities $\pm\frac{3}{2}$), they would be completely irrelevant for the purposes of collider physics. In our discussion of the GMSB model we saw, however, that the amplitudes for decays to the longitudinal components of the gravitino with helicities $\pm\frac{1}{2}$ are enhanced by a factor $E/m_{3/2}$ which is very large if the gravitino is superlight. In this case, sparticle decays to the longitudinal components of the gravitino, which is essentially the goldstino, may be relevant. The NLSP, of course, can only decay into the gravitino. The considerations of this section most directly apply to the GMSB model with a low SUSY breaking scale.

13.8.1 Interactions

The couplings of the gravitino to the fermion–sfermion and to the gauge boson–gaugino system are given by the last term of (10.57a) and the second term of (10.57b), respectively. With $G^i_{\ j} = \delta^i_j + \cdots$ and $f_{AB} = \delta_{AB} + \cdots$ (the ellipsis denotes possible non-minimal terms in these), we find that these couplings can be written as,

$$\mathcal{L} \ni \frac{\mathrm{i}}{\sqrt{2}M_{\mathrm{P}}}\bar{\psi}_\mu \not{D}\mathcal{S}^{i\dagger}\gamma^\mu\psi_{i\mathrm{L}} + \frac{1}{8M_{\mathrm{P}}}\bar{\lambda}_A\gamma^\rho\sigma^{\mu\nu}\psi_\rho F_{A\mu\nu} + \quad \text{h.c.}, \tag{13.30a}$$

where we have inserted the appropriate factors of M_{P}.

In principle, these couplings allow us to evaluate rates for sparticle decays to gravitinos. However, because of the unfamiliarity with manipulating the vector–spinor wave functions of spin $\frac{3}{2}$ particles, it is convenient to work only with the familiar spin $\frac{1}{2}$ goldstino that has been dynamically rearranged by the super-Higgs mechanism, and now forms the helicity $\pm\frac{1}{2}$ components of the gravitino. Then, just as W and Z interactions at high energies can be approximated by the interactions of their longitudinal components (the Goldstone bosons), so too can gravitino interactions be approximated by the interactions of the goldstino fields which they have absorbed by the super-Higgs mechanism.[17] But, we have already obtained the coupling of the goldstino to the chiral supermultiplet. Comparing the first term of (13.30a) with the goldstino coupling in (7.28), we see that the gravitino field can, in the high energy limit, be well approximated by

$$\psi_\mu \to \sqrt{\frac{2}{3}}\frac{1}{m_{3/2}}\partial_\mu\tilde{G}, \tag{13.30b}$$

[17] The goldstino–gravitino equivalence, which was formally established by R. Casalbuoni *et al.*, *Phys. Lett.* **B215**, 313 (1988), ought to be an excellent approximation for decays of 100 GeV sparticles into eV, keV or even GeV scale gravitinos.

https://doi.org/10.1017/9781009289801.014 Published online by Cambridge University Press

where we have used (10.67a) to eliminate the auxiliary field VEV in favor of the gravitino mass, and denoted the goldstino field (previously denoted by ψ_g) by $\tilde{G}$.[18] With this substitution, the interaction Lagrangian (13.30a) becomes

$$\mathcal{L} \ni \sqrt{\frac{2}{3}} \frac{1}{M_{\rm P} m_{3/2}} \left[\frac{1}{8} \bar{\lambda}_A \gamma^\rho \sigma^{\mu\nu} \left(\partial_\rho \tilde{G} \right) F_{A\mu\nu} - \frac{\mathrm{i}}{\sqrt{2}} \bar{\psi}_{i\mathrm{L}} \gamma^\mu \not{D} \mathcal{S} \partial_\mu \tilde{G} \right] + \quad \text{h.c.} \tag{13.30c}$$

The first term in (13.30c) clearly contains the coupling of the goldstino (or equivalently, helicity $\pm\frac{1}{2}$ gravitinos in the high energy limit) to gauginos and gauge bosons, while the second contains the corresponding couplings to the sfermion–fermion or the Higgs boson–higgsino pairs. Note, however, that when the Higgs fields are set equal to their VEV, even the second term contains (via the gauge covariant derivative) couplings of the goldstino to the vector boson–higgsino pair.[19]

These couplings can be used to obtain the interactions that are dominantly responsible for the decays $\widetilde{Z}_i \to \gamma \tilde{G}$ (from the first term alone) or $\widetilde{Z}_i \to Z \tilde{G}$, as well as the interactions that lead to the decay $\widetilde{W}_i \to W \tilde{G}$. The second term yields interactions that lead to the decay of a neutralino (chargino) into a neutral (charged) Higgs boson and a gravitino, as well as to sfermion decays, $\tilde{f}_{1,2} \to f \tilde{G}$. Usually the branching fraction for these gravitino decay modes is significant only for the decay of the NLSP, with the gravitino being the LSP, as is the case in GMSB models with a low SUSY breaking scale.

To evaluate the couplings responsible for $\widetilde{Z}_i \to \gamma \tilde{G}$, we write out the first term in (13.30c) for the neutral $U(1)_{\rm Y}$ and neutral $SU(2)_{\rm L}$ gauge and gaugino fields:

$$\begin{aligned} \mathcal{L} \ni \sqrt{\frac{2}{3}} \frac{1}{8 M_{\rm P} m_{3/2}} \big[& \bar{\lambda}_0 \gamma^\rho \sigma^{\mu\nu} \partial_\rho \tilde{G} (\partial_\mu B_\nu - \partial_\nu B_\mu) \\ & + \bar{\lambda}_3 \gamma^\rho \sigma^{\mu\nu} \partial_\rho \tilde{G} (\partial_\mu W_{3\nu} - \partial_\nu W_{3\mu}) \big] + \quad \text{h.c.}, \end{aligned}$$

and substitute $B_\mu = \sin\theta_{\rm W} Z_\mu + \cos\theta_{\rm W} A_\mu$, $W_{3\mu} = \sin\theta_{\rm W} A_\mu - \cos\theta_{\rm W} Z_\mu$, $\lambda_0 = \sum_i v_4^{(i)} (\mathrm{i}\gamma_5)^{\theta_i} \widetilde{Z}_1$, and $\lambda_3 = \sum_i v_3^{(i)} (\mathrm{i}\gamma_5)^{\theta_i} \widetilde{Z}_i$ to obtain

$$\mathcal{L}_{\widetilde{Z}_i \gamma \tilde{G}} = \sqrt{\frac{2}{3}} \frac{1}{4 M_{\rm P} m_{3/2}} (v_4^{(i)} \cos\theta_{\rm W} + v_3^{(i)} \sin\theta_{\rm W}) \overline{\widetilde{Z}}_i (\mathrm{i}\gamma_5)^{\theta_i} \gamma^\rho \sigma^{\mu\nu} \partial_\rho \tilde{G} (\overleftrightarrow{\partial}_\mu A_\nu). \tag{13.31a}$$

In arriving at this we have used the fact that the Majorana properties of the goldstino and neutralinos imply that the Hermitian conjugate term is identical to the original term, accounting for a factor 2. For the $\widetilde{Z}_i Z \tilde{G}$ interaction, both terms in Eq. (13.30c)

[18] This was first pointed out by P. Fayet, *Phys. Lett.* **B70**, 461 (1977).

[19] We will leave it to the reader to check that this contribution vanishes for the photon as it must since the VEVs leave the electromagnetic gauge invariance unbroken.

https://doi.org/10.1017/9781009289801.014 Published online by Cambridge University Press

contribute, and the coupling is given by

$$\mathcal{L}_{\tilde{Z}_i Z\tilde{G}} = \sqrt{\frac{2}{3}}\frac{1}{4M_{\rm P}m_{3/2}}\Big[(v_4^{(i)}\sin\theta_{\rm W} - v_3^{(i)}\cos\theta_{\rm W})\overline{\overline{Z}}_i(\mathrm{i}\gamma_5)^{\theta_i}\gamma^\rho\sigma^{\mu\nu}\partial_\rho\tilde{G}\overset{\leftrightarrow}{\partial}_\mu Z_\nu$$
$$+ 2M_Z(\mathrm{i})^{\theta_i}(\sin\beta v_1^{(i)} - \cos\beta v_2^{(i)})\overline{\overline{Z}}_i\Gamma\gamma^\mu\gamma^\nu\partial_\mu\tilde{G}Z_\nu\Big], \qquad (13.31b)$$

where $\Gamma = 1$ (γ_5) for $\theta_i = 0$ (1).

The couplings of neutralinos to the goldstino and neutral Higgs bosons can be worked out from the second term in (13.30c) by substituting the higgsinos and the Higgs fields with definite hypercharges in terms of the corresponding mass eigenstate fields. We then find the neutralino–Higgs boson–goldstino interactions:

$$\mathcal{L}_{\tilde{Z}_i\phi\tilde{G}} = \kappa_\phi\overline{\overline{Z}}_i\frac{1+\gamma_5}{2}\gamma^\mu\gamma^\nu\partial_\mu\tilde{G}\partial_\nu\phi + \quad \text{h.c.}, \qquad (13.32a)$$

where $\phi = h,\ H$, and A, and

$$\kappa_h = -\frac{(\mathrm{i})^{\theta_i+1}}{\sqrt{6}M_{\rm P}m_{3/2}}[v_1^{(i)}\cos\alpha + v_2^{(i)}\sin\alpha], \qquad (13.32b)$$

$$\kappa_H = -\frac{(\mathrm{i})^{\theta_i+1}}{\sqrt{6}M_{\rm P}m_{3/2}}[-v_1^{(i)}\sin\alpha + v_2^{(i)}\cos\alpha], \quad \text{and} \qquad (13.32c)$$

$$\kappa_A = -\frac{(\mathrm{i})^{\theta_i+2}}{\sqrt{6}M_{\rm P}m_{3/2}}[v_1^{(i)}\cos\beta + v_2^{(i)}\sin\beta]. \qquad (13.32d)$$

Exercise *Using the Majorana properties of the neutralino and goldstino fields, verify that these couplings can be rewritten as,*

$$\mathcal{L}_{\tilde{Z}_i\phi\tilde{G}} = \overline{\overline{Z}}_i\left[\frac{\kappa_\phi + \kappa_\phi^*}{2} + \frac{\kappa_\phi - \kappa_\phi^*}{2}\gamma_5\right]\partial_\mu\tilde{G}\partial_\nu\phi. \qquad (13.33)$$

Notice that because κ_ϕ is either real or imaginary, the interaction is either scalar or pseudoscalar. This form of the coupling is, therefore, more convenient for evaluating the partial widths for the decays $\widetilde{Z}_i \to \phi\tilde{G}$.

Finally, the last term in (13.30c) also gives the couplings of the goldstino to fermion–sfermion pairs. These can be written as

$$\mathcal{L}_{f\tilde{f}\tilde{G}} = -\frac{\mathrm{i}}{\sqrt{3}}\frac{1}{M_{\rm P}m_{3/2}}\left[\bar{\psi}_f\frac{1+\gamma_5}{2}\gamma^\mu\gamma^\nu\partial_\nu\tilde{f}_{\rm L} + \bar{\psi}_{F^c}\frac{1+\gamma_5}{2}\gamma^\mu\gamma^\nu\partial_\nu\tilde{f}_{\rm R}^\dagger\right]\partial_\mu\tilde{G}$$
$$+ \quad \text{h.c.},$$

where ψ_f (ψ_{F^c}) are, as usual, Majorana spinors whose left-handed components annihilate the left-handed $SU(2)_{\rm L}$ doublet fermion, (left-handed $SU(2)_{\rm L}$ singlet

https://doi.org/10.1017/9781009289801.014 Published online by Cambridge University Press

antifermion) and the SM Dirac fermion is given by

$$f = \frac{1-\gamma_5}{2}\psi_f + \frac{1+\gamma_5}{2}\psi_{F^c}.$$

Writing this Lagrangian with the Hermitian conjugate of the second term, and once again using the Majorana nature of the spinors we find that,

$$\mathcal{L}_{f\tilde{f}\tilde{G}} = -\frac{\mathrm{i}}{\sqrt{3}}\frac{1}{M_{\mathrm{P}} m_{3/2}}\left[\bar{f}\frac{1+\gamma_5}{2}\gamma^\mu\gamma^\nu\partial_\nu\tilde{f}_{\mathrm{L}} - \bar{f}\frac{1-\gamma_5}{2}\gamma^\mu\gamma^\nu\partial_\nu\tilde{f}_{\mathrm{R}}\right]\partial_\mu\tilde{G} + \quad \text{h.c.} \tag{13.34a}$$

Using this, we can readily obtain the goldstino interactions with the sfermion mass eigenstates,

$$\mathcal{L}_{f\tilde{f}_i\tilde{G}} = -\frac{\mathrm{i}}{\sqrt{3}M_{\mathrm{P}} m_{3/2}}\left[\bar{f}(\cos\theta_f P_{\mathrm{R}} + \sin\theta_f P_{\mathrm{L}})\gamma^\mu\gamma^\nu\partial_\mu\tilde{G}\partial_\nu\tilde{f}_1 + \bar{f}(\sin\theta_f P_{\mathrm{R}} - \cos\theta_f P_{\mathrm{L}})\gamma^\mu\gamma^\nu\partial_\mu\tilde{G}\partial_\nu\tilde{f}_2\right] + \quad \text{h.c.} \tag{13.34b}$$

The goldstino–tau–stau coupling leads to the dominant decay of the lighter stau in mGMSB models with the gravitino as the LSP and $\tilde{\tau}_1$ as the NLSP.

13.8.2 NLSP decay to a gravitino within the mGMSB model

Within the mGMSB framework, as we saw in Fig. 11.5 for the number of messenger generations $n_5 = 1$ and $\tan\beta$ not too large, the lightest neutralino tends to be the NLSP. Since gaugino masses scale with n_5 while scalar masses scale with $\sqrt{n_5}$, the lighter stau becomes the NLSP for larger values of n_5. If $\tan\beta$ is small to moderate, the tau Yukawa coupling is small and $\tilde{e}_{\mathrm{R}}$ and $\tilde{\mu}_{\mathrm{R}}$ are roughly degenerate with $\tilde{\tau}_1$, and we have the so-called co-NLSP scenario (region 3 of this figure).

The NLSP dominantly decays into a gravitino and a SM particle. It is straightforward to work out the partial widths for these two-body decays using the interactions presented in the last section. For a neutralino NLSP lighter than h or the Z boson, $\widetilde{Z}_1 \to \gamma\tilde{G}$ is the only allowed two-body decay.

Exercise *Starting with the interaction in (13.31a), show that the width for the decay $\widetilde{Z}_i \to \gamma\tilde{G}$ is given by,*

$$\Gamma(\widetilde{Z}_i \to \gamma\tilde{G}) = \frac{(v_4^{(i)}\cos\theta_{\mathrm{W}} + v_3^{(i)}\sin\theta_{\mathrm{W}})^2 m_{\widetilde{Z}_i}^5}{48\pi\, m_{3/2}^2 M_{\mathrm{P}}^2}. \tag{13.35}$$

Here, we have neglected the gravitino mass (except in the goldstino coupling, of course).

https://doi.org/10.1017/9781009289801.014 Published online by Cambridge University Press

You may find it helpful to use the identity,

$$\gamma^\rho \sigma^{\mu\nu} = 2\mathrm{i}(g^{\rho\mu}\gamma^\nu - g^{\rho\nu}\gamma^\mu) + \sigma^{\mu\nu}\gamma^\rho$$

and use $\tilde{G}_\mu \gamma^\mu u(\tilde{G}) = 0$ *for the massless on-shell goldstino.*

If $m_{\widetilde{Z}_1}$ is large enough, its decays to Z as well as Higgs bosons may also be accessible. The partial widths for these two-body decays of the neutralino are listed in (B.67)–(B.69a) of Appendix B. Since this NLSP is mainly bino-like within the mGMSB model, it has large couplings to the hypercharge gauge boson, and as a result the decay $\widetilde{Z}_1 \to \gamma\tilde{G}$ dominates the decay $\widetilde{Z}_1 \to Z\tilde{G}$ for both dynamical as well as kinematic reasons. Decays to Higgs bosons are strongly suppressed. In non-minimal scenarios, the decays $\widetilde{Z}_1 \to h\tilde{G}$ or $\widetilde{Z}_1 \to Z\tilde{G}$ may be dominant.[20]

The $\widetilde{Z}_1 \to \gamma\tilde{G}$ decay rate depends on $m_{3/2}$, which is independent of other sparticle masses. Recall that in the mGMSB framework, the gravitino mass, and hence the NLSP decay rate, is controlled by the parameter C_{grav}. If $m_{3/2}$ is large enough, then the $\widetilde{Z}_1$ can be very long-lived. The mean decay length for a $\widetilde{Z}_1$ with fractional velocity $\beta_{\widetilde{Z}_1}$ is given by

$$\begin{aligned} d(\mathrm{cm}) &= \beta_{\widetilde{Z}_1}\gamma_{\widetilde{Z}_1} c\tau_{\widetilde{Z}_1} \\ &= \frac{10^{-2}}{(v_4^{(i)}\cos\theta_{\mathrm{W}} + v_3^{(i)}\sin\theta_{\mathrm{W}})^2}(E^2/m^2_{\widetilde{Z}_1} - 1)^{1/2}\left(\frac{100\ \mathrm{GeV}}{m_{\widetilde{Z}_1}}\right)^5\left(\frac{\sqrt{\langle F\rangle}}{100\ \mathrm{TeV}}\right)^4. \end{aligned} \tag{13.36}$$

Remember that $\langle F\rangle$ is the true SUSY breaking scale (not the corresponding scale $\langle F_S\rangle$ in the messenger sector). For $m_{\widetilde{Z}_1} \sim 100$ GeV, the decay length mainly varies with the SUSY breaking scale $\langle F\rangle$ and can range from microns to kilometers and beyond, depending on $\langle F\rangle$. In a collider detector, the NLSP may have a decay vertex displaced from the interaction region, or may even decay outside of the detector. Thus, one of the signatures considered for GMSB models is the presence of hard isolated photons plus missing energy in collider events, where the photon induced EM shower may not point back to the interaction vertex. Indeed, a determination of the lifetime of the NLSP from its decay length distribution would yield the fundamental underlying SUSY scale. For this purpose, the higher order $\widetilde{Z}_1 \to e^+e^-\tilde{G}$ decay may be more suitable for experimental reasons.

Finally, if the stau is the NLSP in the GMSB model, it would decay via,

$$\tilde{\tau}_1 \to \tau\tilde{G} \tag{13.37}$$

[20] See, e.g., K. Matchev and S. Thomas, *Phys. Rev.* **D62**, 077702 (2000).

https://doi.org/10.1017/9781009289801.014 Published online by Cambridge University Press

with a rate given by (B.60). If other flavors of sleptons are also only marginally lighter than the stau NLSP (region 3 of Fig. 11.5 where $m_{\tilde{\ell}_1} - m_{\tilde{\tau}_1} < m_\tau$), the decays (13.16a) are kinematically forbidden, and $\tilde{\ell}_1 \to \ell\tilde{G}$ or via (13.16b), depending on the value of $C_{\rm grav}$. The rates for stau decays to gravitinos are comparable to the corresponding decay rate of a neutralino NLSP of the same mass. Hence, the charged NLSP might again be sufficiently long-lived, and (depending on its β) a highly ionizing track, terminating in a kink or a jet, may provide a characteristic signature.

https://doi.org/10.1017/9781009289801.014 Published online by Cambridge University Press